UNCLASSIFIED

AD 290 519

Reproduced
by the

ARMED SERVICES TECHNICAL INFORMATION AGENCY
ARLINGTON HALL STATION
ARLINGTON 12, VIRGINIA
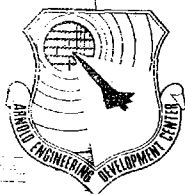
UNCLASSIFIED

NOX

THE DRAG OF SPHERES IN RAREFIED HYPERVELOCITY FLOW

By

Max Kinslow and J. Leith Potter

von Kármán Gas Dynamics Facility

ARO, Inc.

TECHNICAL DOCUMENTARY REPORT NO. AEDC-TDR-62-205

December 1962

AFSC Program Area 750A, Project 8953, Task 895306

ARNOLD ENGINEERING DEVELOPMENT CENTER

AIR FORCE SYSTEMS COMMAND

UNITED STATES AIR FORCE

THE DRAG OF SPHERES IN RAREFIED
HYPERVELOCITY FLOW

By

Max Kinslow and J. Leith Potter

von Kármán Gas Dynamics Facility

ARO, Inc.

a subsidiary of Sverdrup and Parcel, Inc.

FOREWORD

ABSTRACT

Through use of the low-density, hypervelocity wind tunnel of the von
Kármán Gas Dynamics Facility, drag of spheres has been measured under
hypersonic, cold-wall $(T_w \ll T_o)$, support-free conditions in a nonreacting
(vibration frozen) flow. Data were obtained for a nominal free-stream
Mach number of 11 and for Reynolds numbers from 1 to 10 based on condi-
tions immediately downstream of the bow shock and sphere diameter.
These data were supplemented by measurements at a nominal Mach num-
ber of 10 where a conventional balance was used, and Reynolds numbers
downstream of the shock as high as 10^4 were investigated in the cold-wall
condition.

The experimental results have been analyzed both from the point of
view of continuum flow with second-order viscous effects, and from the
standpoint of a noncontinuum concept, taking account of first collisions
between reemitted and free-stream molecules. In the former case, a
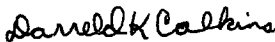drag coefficient representation of the form

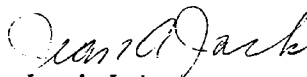$$C_D = C_{D_{inviscid}} + K_1/\sqrt{Re_2} + K_2/Re_2$$

is shown to fit the data very closely when K_1 and K_2 are allowed to be
functions of free-stream Mach number and wall-to-total enthalpy ratio.
Data from investigations at the University of California, University of
Toronto, and Jet Propulsion Laboratory have been used to enlarge the
present study and, in particular, to support the evaluation of K_1 which
represents the influences of vorticity, curvature, thick boundary layer,
slip, and temperature jump. In all cases, K_2 was found to be negative
in sign.

The new first-collision analysis is numerically indeterminant be-
cause of the lack of a method for explicit calculation of mean free path
in real, polyatomic gases with consideration of intermolecular forces.
However, the form of the derived equation for $C_D/C_{D_{free\ molecular}}$ appears
to fit the experimental data over a considerable range of Knudsen num-
bers if a free constant is used in the expression for mean free path. It
is considered that this constant is influenced by the type of intermolecu-
lar and gas-solid interactions occurring. Fully accommodated, diffusely
reflected surface interaction was assumed in the analysis.

CONTENTS

TABLE

ILLUSTRATIONS

NOMENCLATURE

A	$\sqrt{(r/\lambda_w)^2 - (R/\lambda_w)^2}$
a	Speed of sound, $\sqrt{\gamma R T}$
B	$r/\lambda_w - R/\lambda_w$
b	Constant
C_1, C_2, C_3	Constants
C_D	Drag coefficient, defined by Eq. (3)
$C_{D_{fm}}$	Free-molecule drag coefficient, defined by Eq. (53)
C_{D_i}	Inviscid drag coefficient
C_p	Specific heat of gas at constant pressure
C_v	Specific heat of gas at constant volume
D	Drag of sphere
d	Diameter of sphere
dA	Elemental area of surface
$d\omega$	Incremental solid angle
$-Ei(-x)$	Generalized exponential integral, $\displaystyle\int_x^\infty \frac{e^{-x}}{x}\, dx$
$\text{erf } x$	Error function
$G(v/\bar{v})$	Function, defined by Eq. (43)
g	Acceleration due to gravity
H_w	Enthalpy parameter, defined by Eq. (7)
h	Enthalpy
K	Thermal conductivity
K_1, K_2	Constants
K_n	Knudsen number
k	Boltzmann constant
ℓ	Coordinate measured from a point on a surface to a point in space
M	Mach number
m	Mass of a molecule
$N(\ell)$	Number of molecules

ix

n	Number density of molecules
$n(v)$	Number density of molecules in velocity, position coordinates
P	A point in space
P_r	Prandtl number
R	Radius of sphere
R	Gas constant, k/m
R_e	Reynolds number, $Ud\rho/\mu$
r	Coordinate from center of sphere
S	Molecular speed ratio, $U/\sqrt{2RT}$
T	Temperature
U	Velocity
v	Velocity of a molecule
$\bar{v}$	Mean molecular speed, $\sqrt{8RT/\pi}$
$\bar{v}_w$	Mean velocity of molecule leaving a surface
x	Axial coordinate
y	Vertical coordinate
$\alpha(v)$	Collision probability of a molecule with speed v, $1/\lambda(v)$
γ	Ratio of specific heats, C_p/C_v
Δx	Difference between axial coordinates
η	Collision rate density between wall and free-stream molecules
θ	Angle between normal to dA and the free-stream velocity vector (see Fig. 10)
λ	Mean free path
$\lambda(v)$	Mean free path of molecules with speed v
λ_w	Mean free path of a molecule reemitted with speed $\bar{v}_w$ relative to free-stream molecules
$\bar{\lambda}_w$	Mean free path of reemitted molecules relative to free-stream molecules
μ	Viscosity

ρ	Mass density
σ	Effective molecular diameter
r	Shear stress
ϕ	Angle between the normal to dA and the incident or reemitted path (or velocity vector) of a molecule (see Fig. 10)

SUBSCRIPTS

o	Total or isentropic stagnation condition
2	Condition immediately downstream of normal shock
i	Incident molecules
s	Scattered molecules
w	Wall condition
∞	Free-stream condition

1.0 INTRODUCTION

It is well known that the aerodynamic drag of spherical bodies in hypersonic flow is more than doubled when the flow passes from a condition characterized by "thin" boundary layers to a condition of free-molecular flow. The first condition usually is identified with large Reynolds numbers, R_e, whereas the flow parameter associated with the second condition is Knudsen number, K_n. A relation between these parameters and the Mach number, M, was derived by von Kármán who found

$$K_n \sim M/R_e \tag{1}$$

The constant of proportionality is approximately 1.49 for air at moderate temperature and pressure.

The drag coefficients of hypersonic spheres at both very high Knudsen numbers (> 10) and very low Knudsen numbers $(< 10^{-4})$ are known to at least a moderate degree of accuracy, although there is uncertainty regarding the accommodation coefficients in free-molecular flows. In the intermediate range of Knudsen numbers, where neither analysis nor experiment has fully answered the question, significant contributions have been made by both approaches. Some of the more recent work is reported in Refs. 1-16, where sources of additional material also are given.

With regard to the high Knudsen number or near-free-molecular flow regime, the obstacles to analytical solution arise chiefly from the lack of exact knowledge of the behavior of molecules after impact on the sphere and the mathematical complexity of the flow model when interactions between free-stream and reflected molecules become important. In the continuum, viscous-interaction regime of small Knudsen numbers the usual difficulty of dealing with flows characterized by thick boundary layers in the presence of vorticity, curvature, displacement, slip, and temperature jump presents the main obstacle.

The reason that experimental data have not been presented for the entire intermediate regime is basically the lack of facilities capable of duplicating all the conditions of flow desired for the investigation. Nonetheless, experimental data provide the more significant part of the knowledge of sphere drag in the region $10^{-4} \leq K_{n_\infty} \leq 10$, where K_{n_∞} is based on free-stream conditions and sphere diameter.

Manuscript released by authors October 1962.

1

The Low-Density, Hypervelocity (LDH) Wind Tunnel (Ref. 7) of the von Kármán Gas Dynamics Facility (VKF), Arnold Engineering Development Center (AEDC), Air Force Systems Command (AFSC), US Air Force, has been used to extend previous experimental studies of drag of spheres in low-density flow. Using the LDH Tunnel, drag data have been taken under hypersonic, cold-wall ($T_w \ll T_o$) support-free conditions which are described later.

These and earlier data from other sources have been examined in regard to both continuum and noncontinuum fluid flow behavior. The purpose of this report is to present the new data and analyses.

2.0 EXPERIMENTAL PROCEDURE AND DATA

2.1 LDH WIND TUNNEL

The LDH Tunnel (Fig. 1) is of the continuous type, with the gas heated by an electric arc or plasma generator. Test section conditions have been determined from analysis of impact pressure, local mass flow rate, calorimeter, and static pressure measurements. A description of the facility is contained in Ref. 7. Briefly, the tunnel consists of a d-c arc-heater, stilling chamber, conical nozzle of 15-deg half angle, test chamber with instrumentation, diffuser, and pumping system. Additional information on the nozzle flow is contained in Refs. 17 and 18.

Measurements of total enthalpy at the nozzle throat by calorimetry agree closely with total enthalpy computed on the basis of measured mass flow rate, total pressure, sonic throat area, and the assumption of thermodynamic equilibrium in the fluid upstream of the throat. However, on the basis that computed relaxation lengths for molecular vibration downstream from the throat are from 10^2 to 10^4 times local nozzle radius, all theoretical evidence indicates frozen flow from the throat onward. Thus, test section flow characteristics are based on sudden freezing of the flow at the throat.

Operating conditions for this experiment follow:

Gas	=	Nitrogen			
Nominal Nozzle Station	=	1.0 in. downstream of exit			
Dynamic Pressure, psfa	=	2.12	2.51	3.16	3.31
Total Enthalpy, Btu/lb	=	871	1110	1560	1760
Total Temperature, °R	=	3150	3960	5400	6030
Mach Number	=	10.8	10.6	10.7	10.6
Unit Re_∞/in.	=	466	426	344	301
Unit Re_2/in.	=	47.0	42.6	37.6	34.7
Mean Free Path, λ_∞, in.	=	0.0508	0.0548	0.0686	0.0776

using $\lambda_\infty = 1.26 \sqrt{\gamma} \, \mu_\infty / (\rho_\infty a_\infty)$

2

2.2 SPHERE DRAG MEASUREMENT

2.2.1 Free-Fall Method

For the smaller spheres (0.0313 to 0.375-in.-diam) a free-fall technique was used to determine drag. The models were injected into the test stream and their trajectories determined using a photographic technique whereby a time exposure was made of the moving model which was illuminated by an interrupted light source. Spheres with diameters of 0.0625 to 0.375-in. were dropped into the test section by an electromagnet from a position just above the test section. However, the spheres had a tendency to retain some residual magnetism, thereby making release of the smaller spheres difficult. In order to facilitate the release of the smaller spheres, a solenoid was wound near the end of a short length of copper tubing. With the solenoid energized, test spheres of 0.0313 to 0.156-in. diam could be suspended within the tubing. By deenergizing the solenoid, the models were free to fall down the tubing. The end of the tubing was bent so that the models could be injected into the test stream at the appropriate angle.

The light source used to illuminate the spheres during their flight through the test section was a 1000-watt projector lamp. The light intensity was modulated using a rotating disc containing holes drilled around the periphery. The disc was rotated by a high-speed motor so that the light at the test section could be interrupted at rates up to 1000 per second. By taking a time exposure of the test section, the trajectory of the sphere was recorded photographically at equal time intervals during its flight.

Since the test section is about 1-in. in diameter, a telephoto lens was used so that the photograph of the test region could be magnified for easier data reduction. An example is shown in Fig. 2.

Surface temperatures of the spheres tested by the free-flight method were approximately 0.1 total temperature.

2.2.2 Axial-Force Balance

A smaller amount of data was obtained earlier for spheres of 0.265 to 0.686-in. diam by means of an external, sting-type, water-cooled, axial-force balance capable of measuring forces on the order of 0.001 lb. Temperatures of the spheres on this balance were somewhat greater than in the free-fall case, although $T_w < T_o$, and minimum sphere size was limited to approximately 0.25 in. A photograph of this balance installed in the LDH tunnel is shown in Fig. 3.

3

The test spheres were steel ball bearings with a 0.1-in. hole drilled to admit the sting support. The spheres were uncooled except for radiation from the surface and conduction through the sting mount. Wall temperature of the spheres reached approximately 0.3 total temperature.

It should be noted that these are essentially the same data first published in Ref. 7, but the points now have been shifted slightly because of the use of a new source (Ref. 19) for viscosity of nitrogen at high temperatures. Good agreement is evident in comparing free-fall and balance measurements.

A small quantity of new data at higher Reynolds numbers from the 50-Inch Mach 10 Tunnel (C) in VKF is included. These were obtained by use of the same axial-force balance used in the LDH Tunnel.

2.3 DATA REDUCTION

The data from the free-fall tests were obtained in the form of photographs (Fig. 2) which showed the trajectory of the sphere at equal time increments. The two larger light spots in the example shown in Fig. 2 were used to orient the photograph, since the Polaroid back to the camera could be moved slightly relative to the tunnel. These position points were obtained by a double exposure. One exposure was made of the path of the sphere and the other of the two reference light sources which could be positioned on the nozzle exit before or after a run. The position points were located approximately 0.5 in. above and below the tunnel centerline and 0.5 in. from the nozzle exit.

The coordinates of each trajectory point on a film were read using graph paper for a grid and using the position points for alignment. Initially it was deemed desirable to reduce the x, y coordinates obtained from the photograph to an acceleration in the x-direction by using the known acceleration of gravity as a reference. Writing d^2x/dt^2 in terms of the x, y coordinates with y a function of time gives

$$\frac{d^2 x}{dt^2} = \frac{dx}{dy} \frac{d^2 y}{dt^2} + \left(\frac{dy}{dt}\right)^2 \frac{d^2 x}{dy^2}$$

where d^2y/dt^2 is the acceleration due to gravity, g.

The least-squares method was used to give $x = f(y)$ for polynomials of various degree, from which dx/dy and d^2x/dy^2 were determined. The term dy/dt was found by fitting a straight line through the values of

4

$(y - gt^2/2)$ plotted as a function of t, i.e., if

$$y - \frac{g}{2} t^2 = y_0 + bt$$

then

$$\frac{dy}{dt} = b + gt$$

Values of d^2x/dt^2 were determined as a function of time across the test section. However, since $x = f(y)$ is not a polynomial for a body in a uniform force field, the value obtained for d^2x/dt^2 was not constant throughout the test section. Therfore, it was concluded that a more straight-forward method should be used.

Next, the difference in axial coordinates of adjacent points, Δx, was plotted as shown in Fig. 4. The slope of the line through these points is proportional to the acceleration of the sphere in the axial direction. * The constant of proportionality between this slope and the sphere acceleration was obtained by combining the known time between successive points on the photograph and the known scale factor of the photograph. The choice was made to combine the time and position scales into one constant so that graph paper could be used to read coordinates and the points could be plotted simply as a function of point number.

Using Newton's second law in the form

$$D = m \, d^2x/dt^2 \tag{2}$$

the total drag force on a sphere was determined from its acceleration and its mass. The mass was determined by using an analytical balance for weighing several spheres of the same size and then taking an average. Values of the drag coefficient, C_D, were obtained for the sphere using the definition

$$C_D = \frac{D}{\frac{1}{2} \rho_\infty U_\infty^2 A} \tag{3}$$

where A is the cross-sectional area of the sphere. Table 1 summarizes the conditions and results of these tests.

Reduction of data from the axial-force balance was accomplished by the usual, well-known procedure involving use of a calibration curve obtained by static calibration of the balance using known drag loads.

---

*It can be shown that this finite difference method for obtaining the acceleration of a model in a uniform force field gives a result equal to that from the second derivative of the position-time curve.

3.0 ANALYSIS

3.1 THE SPHERE IN LOW-DENSITY, CONTINUUM FLOW

It is a generally accepted approximation that the drag coefficient of a sphere in supersonic, low-density but continuum flow may be expressed as the sum of its drag coefficient at essentially infinite Reynolds number, C_{D_i}, plus the contribution from skin friction, plus a third term representing the combined influences of vorticity, slip, temperature jump, and non-negligible ratios of boundary-layer thickness to sphere radius, cf Refs. 11, 20-22.

Consideration of only the dominant inviscid and first-order friction terms led Chahine (Ref. 13) to the result (in the present nomenclature),

$$C_D = C_{D_i} + \frac{9 \, f_w''/8}{\sqrt{Re_2 \, \rho_\infty/\rho_2}} \tag{4}$$

where f_w'' is the shear function given by Cohen and Reshotko in Ref. 23. The 9/8 is an empirically derived constant apparently based on data taken under conditions where $M_\infty = 4$, $T_w \geq T_2$, and $T_2 = T_0$. Chahine treats f_w'' as a constant, taking the stagnation point value.

Rott and Wittenbury in Ref. 11 considered all the factors mentioned above and arrived at the expression (again using present nomenclature):

$$\tau/(\rho_2 U_\infty \sin \theta) = C_1 \sqrt{(\lambda_2/R)(a_2/U_\infty)} + C_2 (\lambda_2/R)(a_2/U_\infty) + \cdots \tag{5}$$

where

$$C_1 = f_1 \, [\rho_\infty/\rho_2, \, \mu(T), \, P_r, \, T_w/T_0, \, \ldots \ldots \ldots]$$

$$C_2 = f_2 \, (\text{vorticity, displacement, curvature, slip, } \cdots)$$

The form of Eq. (5) may be made more nearly similar to that of Eq. (4) by using the following relations:

$$\rho_\infty U_\infty = \rho_2 U_2$$

$$R/\lambda_2 = 1/K_{n_2} = \text{const. } Re_2/M_2$$

$$a_2/U_\infty = \text{const. } (\rho_\infty/\rho_2) \, R/(\lambda_2 \, Re_2)$$

$$C_f = 2 \, \tau/(\rho_\infty U_\infty^2)$$

Substituting the above relations into Eq. (5) yields

$$C_f = 2 \sin \theta \left[\frac{\text{const.}(C_1)}{\sqrt{Re_2 \, (\rho_\infty/\rho_2)}} + \frac{\text{const.}(C_2)}{Re_2} + \ldots \ldots \right]$$

6

If K_1 is regarded as a function of ρ_∞/ρ_2, among other things, then one is led to write

$$C_D \approx C_{D_i} + \frac{K_1}{\sqrt{Re_2}} - \frac{K_2}{Re_2} + \ldots \ldots \tag{6}$$

This is the form indicated by Aroesty (Ref. 16) in discussing the subject, and it is interesting to note his comment that neither the sign nor magnitude of K_2 has been established previously. The "approximately equals" symbol is inserted by the present authors, partly out of consideration of the finite range of validity of the equation and partly because the coefficients K_1 and K_2 are later determined empirically.

A presentation of both the new and the more recent of the previously published measurements of drag of spheres in supersonic and hypersonic flows is given in Figs. 5-7 where Re_2 is used as the parameter. * Curves of the form described by Eq. (6) have been fitted to these data, with C_{D_i} taken from Ref. 24 for corresponding Mach numbers. The values of K_1 and K_2 determined by this process are presented in Figs. 8 and 9 as functions of the enthalpy parameter,

$$H_w = h_w/h_o - 1 \tag{7}$$

because the heat-transfer situation would be expected to be important. However, it is apparent that Mach number or some function thereof exerts an influence on the coefficients.

Although there is the possibility of correlating K_1 and possibly K_2 with known parameters, it must be remembered that base drag could be important at the lower Mach numbers (Refs. 25-26). In view of this, plots of the coefficients as functions of Mach number or density ratio may not be unique for $M_\infty \gtrsim 6$. Therefore, no additional correlations are presented. There is evidence in Figs. 8 and 9 that K_1 and K_2 tend toward dependence on H_w alone at large Mach numbers in the essentially perfect gases represented. One would expect this, excepting effects such as chemical relaxation and ablation which were not present in the tests being discussed.

It is thought that the more conclusive portions of Figs. 8 and 9 are those pertaining to the cold-wall, hypersonic case of $M_\infty > 6$ and $H_w \to -1$, because the influence of base pressure and other Mach number dependent factors must be minimized there. Also, variations about the nominal

---

*The conventional thin shock wave and inviscid shock layer are assumed in computing Re_2, and the sphere diameter is used as the characteristic length.

Mach number in the experiments would have less effect on the data, thereby decreasing scatter and aiding in determining the coefficients.

The situation is less clear in regard to K_2 because it assumes importance only at the lowest Reynolds numbers and some older data do not penetrate sufficiently into that regime. The values of K_2 deduced from the data are consistently negative, which is rather interesting because, to the authors' knowledge, this possibility has not been suggested previously.

Van Dyke (Ref. 27) has calculated an example pertaining to the stagnation region of a sphere with entropy gradient, longitudinal curvature, transverse curvature, slip, and temperature jump considered. He assumed that $M_\infty = \infty$, $Pr = 0.7$, $\mu \sim T$, $H_w = -0.8$, and $\gamma = 7/5$, and neglected the displacement boundary layer. One result, which may be expressed in terms of K_1 and K_2, is, in the present nomenclature,

$$K_2/K_1 \ (\text{at stag. pt.}) = -0.661$$

On the other hand, we find experimentally, for $H_w = -0.8$ and $M_\infty = 11$,

$$K_2/K_1 \ (\text{average}) = -0.57$$

where the negative sign is due to K_2 (average). (The sign of K_2 causes K_1 to be larger than it would be if K_2 were neglected as in Eq. (4).

It should be noted that the terms in the algebraic sum giving K_2/K_1 from Van Dyke's analysis are both positive and negative in sign. Therefore, it is not inconceivable that K_2/K_1 (average) would be less than the stagnation region value or that it would be negative. It may be relevant to add Van Dyke's remark that the effect of entropy gradient calculated by Van Dyke is twice as large as that found by Probstein (Ref. 28), but less than one-half that predicted by Ferri, Zakkay, and Ting (Ref. 29). Also, the Navier-Stokes equations on which Van Dyke's analysis is based may not be valid below $Re_2 = 0(100)$, but the experimentally determined coefficients were strongly influenced by data corresponding to $Re_2 \ll 100$.

In view of the uncertainty that would exist in theoretical estimates of the coefficient K_2 (average), it appears that the experimental values presented here are reasonable. No other experimentally derived values are known to the writers.

It is important to keep in mind that Eq. (6) must fail at sufficiently low Reynolds numbers. This failure may be postponed by inserting additional terms, but that is not possible in the absence of reliable drag data for very nearly free-molecular flow. Finding the subsequent terms does not seem highly important in the cold-wall, hypersonic case since the two terms

identified here are sufficient to the limit of continuum flow where it is then necessary to seek further extensions by means of noncontinuum flow analysis.

3.2 THE SPHERE IN NONCONTINUUM FLOW

3.2.1 Some Comments on Mean Free Path

Often in the study of elementary kinetic theory of gases the gas molecules are approximated by small, perfectly elastic spheres (billiard-ball model). This simplified model naturally leads to the idea of a molecular collision and suggests the concept of a free path between collisions. The mean free path, λ, of these billiard-ball molecules can be expressed as

$$\lambda = 1/\left(\sqrt{2} \, n \, \pi \, \sigma^2 \right) \tag{8}$$

where n is the number density of molecules and σ is the diameter of the molecule.

This equation is of little use for calculating mean free path since σ cannot be determined directly. However, the equation shows that the mean free path for an elastic sphere molecule is a function of gas density only and is inversely proportional to it.

The idea of the billiard-ball molecule can be extended, and expressions for the transport properties of viscosity and thermal conductivity can be obtained. These expressions are, respectively,

$$\mu \sim \rho \, \lambda \, \bar{v}$$

and

$$K \sim \rho \, \lambda \, \bar{v} \, C_v$$

where $\bar{v}$ is the mean molecular speed, ρ the mass per unit volume, and C_v the specific heat at constant volume. The most simplified calculation gives the value of $1/3$ for both constants of proportionality.

More comprehensive analyses have yielded values for the constant of proportionality such as $0.350, 0.310, 0.491,$ and 0.499 in the formula for viscosity. Values for the constant of proportionality in the formula for thermal conductivity vary from 1.10 to 2.52 times greater than those for viscosity.

The many different constants obtainable make the numerical determination of mean free path very questionable. The only encouragement comes from the fact that all analyses give the same general form for the

equations. Other models for the molecule besides the hard sphere also give equations of this form. Any assumed force field between molecules except the billiard-ball type does away with the idea of a rigorous free path. Each molecule is in contact with all other molecules, to some extent, at all times.

The equations mentioned above can be applied to obtain an effective mean free path for each property. Thus, there is obtained an effective mean free path for viscosity and one for thermal conductivity. These two mean free paths are different and vary differently with temperature. These differences can be explained on the grounds that distinctions in different molecular properties are important in defining different effective mean free paths. Viscosity is associated with the transfer of momentum across a plane, and the exchange of momentum during a collision is important, whereas thermal conductivity arises from the exchange of energy during a molecular encounter. Each of the mentioned phenomena is associated with a central type collision. (A collision in which the molecules are only slightly deflected does not exchange an appreciable amount of momentum or energy.) Other phenomena, such as scattering, would place just as much importance upon the glancing collisions. Molecular scattering experiments give mean free paths that are less than half those from viscosity measurements.

These effective mean free paths can be used with Eq. (8) to define molecule diameter or collision cross sections. It is found that the collision cross section decreases with rising temperature. These results are expected for molecules with a force field different from the billiard-ball model. The effect of an increase in temperature is to increase the molecular velocities. A molecule will therefore reside a shorter time in the vicinity of another molecule and experience a correspondingly smaller deflection which is equivalent to a smaller effective collision cross section.

In order to bypass these problems, the viscosity equation may be used to determine the form for the mean free path as a function of temperature, but the constant will be unspecified. In other words, instead of using mean free path as a parameter, $\mu\sqrt{\gamma}/(\rho a)$ may be used. The mean molecular velocity, $\bar{v}$, has been replaced by the speed of sound, a. This may be done because a is directly proportional to $\bar{v}$ for constant ratio of specific heats, γ, and is given by the following equation:

$$a = \sqrt{\frac{\gamma \pi}{8}} \; \bar{v}$$

The choice to replace $\bar{v}$ by a may be justified because the speed of sound appears more frequently in the study of high-speed gas flows, and tabulated values of the speed of sound are readily available for real gases.

The dimension of $\mu\sqrt{\overline{\gamma}}/(\rho a)$ is the same as that of mean free path, i.e., length. This parameter can be ratioed to a body dimension to obtain a dimensionless ratio. Using the sphere diameter, d, for this characteristic dimension, the dimensionless parameter becomes $\mu\sqrt{\overline{\gamma}}/(d\rho a)$. Multiplying both numerator and denominator of this expression by the gas velocity gives

$$Kn \sim \sqrt{\overline{\gamma}}\, M/Re \tag{9}$$

It has been shown that the mean free path of real gas molecules is not uniquely determined. However, in subsequent theoretical developments it is assumed that some effective mean free path exists and that the gas molecules can be treated as elastic spheres. In order to compare a theoretically derived equation with experimental data, a free constant is later introduced in the relationship between mean free path and the quantity,

$$\mu\,\sqrt{\overline{\gamma}}/(\rho a) \tag{10}$$

3.2.2 Interaction of Gas Molecules and a Solid Surface

One of the most difficult problems arising in a kinetic theory discussion of gas flow is that of the interactions between the gas molecules and a solid boundary. The problem of this gas-solid interaction is associated with the reflection or reemission of the molecules from the surface, i.e., how the momentum and energy of the molecules and their different degrees of freedom are accommodated to wall conditions. For polyatomic molecules there is an accommodation for each mode of interaction. Thus, there is an accommodation coefficient of mass, translational energy, vibrational energy, tangential momentum, normal momentum, etc. The reader interested in a detailed discussion of the interaction phenomenon may find several reviews of the subject (cf Ref. 30).

Experimental results indicate that for usual engineering surfaces the actual reflection process is near a diffuse reflection. The equation describing a diffuse molecular reflection with complete accommodation to wall conditions will be developed below.

The number of molecules incident upon an elemental area, dA, per unit time is, from Ref. 31 (See nomenclature and Fig. 10.),

$$n_i \sqrt{\frac{k\,T_i}{2\,\pi\,m}} \left\{ e^{-(S\,\cos\,\theta)^2} + \sqrt{\pi}\,(S\,\cos\,\theta)\left[1 + \mathrm{erf}\,(S\,\cos\,\theta)\right] \right\} dA \tag{11}$$

For the development of diffuse reflection from a surface, it is assumed that the reflection from each incremental surface area is the

same as the effusive flow of a hypothetical gas at wall temperature through an opening replacing the incremental area. The density of this hypothetical gas can be determined from the conservation of molecules.

Kennard (Ref. 32) gives the number of molecules crossing any incremental area within a gas per unit time with speed between v and $v + dv$ within the solid angle, $d\omega$, as

$$n_w \left(\frac{m}{2\pi kT_w}\right)^{3/2} v^3 e^{-\frac{mv^2}{2kT}} \cos\theta \, dv \, d\omega \, dA \qquad (12)$$

In the free-molecule regime the flow of molecules through an opening, dA, is the same as that given in Eq. (12). Integrating over all speeds, the total number of molecules passing (reemitted from) dA within the solid angle, $d\omega$, is

$$n_w \left(\frac{m}{2\pi kT}\right)^{3/2} \cos\phi \, d\omega \, dA \int_0^\infty v^3 e^{-\frac{mv^2}{2kT}} dv = n_w \left(\frac{2kT_w}{m}\right)^{1/2} \left(\frac{\cos\phi \, d\omega \, dA}{2\pi^{3/2}}\right) \qquad (13)$$

Because it is assumed that the flow is reflected symmetrically about the normal to the surface, $d\omega$ may be written as (See Fig. 10.)

$$d\omega = 2\pi \sin\phi \, d\phi \qquad (14)$$

The total number of molecules within the angle ϕ to $\phi + d\phi$ is, substituting Eq. (14) in Eq. (13),

$$n_w \left(\frac{2kT_w}{m}\right)^{1/2} \frac{\cos\phi \sin\phi \, d\phi}{\sqrt{\pi}} \, dA \qquad (15)$$

Integrating Eq. (15) over all directions in which molecules can be reflected from the surface $\left(0 \leq \phi \leq \frac{\pi}{2}\right)$ gives

$$n_w \left(\frac{2kT_w}{\pi m}\right)^{1/2} \frac{dA}{2} \qquad (16)$$

the total number of molecules reflected from the surface. Equating this expression to the number of incident molecules (Eq. (11)) gives a solution for n_w:

$$n_w = n_i \sqrt{\frac{T_i}{T_w}} \left\{ e^{-(S\cos\theta)^2} + \sqrt{\pi} (S\cos\theta) \left[1 + \mathrm{erf} (S\cos\theta) \right] \right\} \qquad (17)$$

12

The mean speed of the reemitted molecules is defined as

$$\bar{v}_w = \frac{n_w \left(\frac{m}{2\pi k T_w}\right)^{3/2} \cos\phi \; d\omega \; dA \int_0^\infty v^4 e^{-\frac{m v^2}{2k T_w}} \; dv}{n_w \left(\frac{m}{2\pi k T_w}\right)^{3/2} \cos\phi \; d\omega \; dA \int_0^\infty v^3 e^{-\frac{m v^2}{2k T_w}} \; dv}$$

or

$$\bar{v}_w = \sqrt{\frac{9}{8} \, \pi \; \frac{kT}{m}} \tag{18}$$

3.2.3 Derivation of Mean Free Path of Reemitted Molecules

In any discussion of free-molecular flow or near-free-molecular flow, the dimensionless ratio of some mean path of gas molecules to some characteristic dimension usually is introduced as a parameter. This dimensionless ratio is, of course, the Knudsen number. One problem that arises in connection with the Knudsen number is that of determining which mean free path is the most significant in the problem at hand. Another important related question is that of the numerical determination of this mean free path. This latter problem was discussed in Section 3.2.1.

The Knudsen number may be based upon a "free-stream" mean free path which is independent of free-stream velocity and body conditions. However, if interference between free-stream and reemitted molecules exists, it is reasonable to seek some mean free path more descriptive of the flow. Since the molecular mean free path is always finite, the molecules reflected from the body will always disturb the free stream to some extent. A criterion for closeness to truly free-molecule flow is the average distance a reflected molecule travels after leaving the body surface before experiencing a collision with a free-stream molecule. This mean free path of reemitted molecules, λ_w, is determined in the remainder of this section.

The velocity, relative to the free stream, of a molecule leaving the body is the vector sum, $v + U_\infty$. The mean free path of a reflected molecule is different from λ_∞ since the velocity is different from the mean thermal velocity in the free stream, $\bar{v}_\infty$. Jeans (Ref. 33) gives the mean free path of molecules with speed, v, in a static gas. This mean free path for a molecule with speed, v, is

$$\lambda(v) = \lambda_\infty \, G(v/\bar{v}_\infty) \tag{19}$$

A graphical representation of this is given in Fig. 11. (The equation of $G(v/\bar{v}_\infty)$ is given later as Eq. (43).)

Therefore, the distance traveled by the reflected molecules is

$$\lambda \left(|v + U_\infty| \right) = \lambda_\infty \, G \left(\frac{v - U_\infty}{\bar{v}_\infty} \right)$$

Notice that this is not the distance from the body, because the body has been moving with velocity U_∞ since the molecule left the surface. The time required to traverse this free path is

$$\frac{\lambda_\infty \, G \left(\frac{|v + U_\infty|}{\bar{v}_\infty} \right)}{|v + U_\infty|}$$

Converting to a coordinate system fixed relative to the body and using the velocity of the reflected molecule and the mean time before a collision as developed above, the mean free path, relative to the body, of a molecule with velocity v is

$$\frac{\lambda_\infty \, G \left(\frac{|v + U_\infty|}{\bar{v}_\infty} \right)}{|v + U_\infty|} \, |v| \tag{20}$$

If it is assumed that the directional distribution of mean free paths is similar for spheres under varying conditions, then a representative free path that is easy to calculate can be chosen. The mean free path easiest to determine and the most important from the standpoint of altering the free stream is the free path of molecules directed upstream into the oncoming flow. Expressed in terms of the average speed of the molecules leaving the surface this reemitted mean free path*, λ_w, becomes

$$\lambda_w = \frac{\lambda_\infty \, G \left(\frac{\bar{v}_w + U_\infty}{\bar{v}_\infty} \right)}{\bar{v}_w + U_\infty} \, \bar{v}_w \tag{21}$$

The mean velocity of molecules leaving the sphere is, from Eq. (18),

$$\bar{v}_w = \sqrt{\frac{9\pi}{8} R \, T_w}$$

---

*Probstein (Ref. 34) defines a mean free path of reemitted molecules relative to incident molecules for a hypersonic Mach number and a highly cooled body. He concludes that this mean free path is the mean free path most significant in the free-molecule flow and near-free-molecular regimes.

14

The free-stream velocity may be written as

$$U_\infty = M_\infty \sqrt{\gamma R T_\infty} \tag{22}$$

and the free-stream, mean thermal velocity is

$$\bar{v}_\infty = \sqrt{\frac{8 R T_\infty}{\pi}} \tag{23}$$

Thus, substituting Eqs. (18), (22), and (23) into Eq. (21) gives the mean free path of molecules reflected from the body with velocity $\bar{v}_w$ and directed upstream:

$$\lambda_w = \lambda_\infty \frac{G \left(\frac{3\pi}{8} \sqrt{\frac{T_w}{T_\infty}} + M_\infty \sqrt{\frac{\gamma\pi}{8}}\right)}{1 + M_\infty \sqrt{\frac{8\gamma}{9\pi}} \left(\frac{T_\infty}{T_w}\right)} \tag{24}$$

Dividing both sides of Eq. (24) by a reference length, one finds

$$Kn_w = Kn_\infty \frac{G \left(\frac{3\pi}{8} \sqrt{\frac{T_w}{T_\infty}} + M_\infty \sqrt{\frac{\gamma\pi}{8}}\right)}{1 + M_\infty \sqrt{\frac{8\gamma}{9\pi}} \left(\frac{T_\infty}{T_w}\right)} \tag{25}$$

Equation (25) is based upon the assumption of complete accommodation of the reemitted molecules to the wall condition. For specular reflection from the surface, $\bar{v}_w$ is equal to the incident velocity, U_∞, and Eq. (21) becomes

$$\lambda_w = \frac{\lambda_\infty}{2} G \left(\frac{2 U_\infty}{\bar{v}_\infty}\right) \tag{26}$$

Independent of the type of molecule reflection, the reflected mean free path is proportional to the free-stream mean free path for constant free-stream conditions and wall temperature, i.e.,

$$Kn_w \sim Kn_\infty \quad \text{for } M_\infty = \text{const. and}$$
$$T_\infty/T_w = \text{const.}$$

Combining this relationship with Eq. (9) gives

$$Kn_w \sim \sqrt{\gamma} \frac{M_\infty}{Re_\infty} \tag{27}$$

The mean free path of molecules emitted from the body and directed upstream will, in general, not equal the mean free path of molecules with

the mean emitted velocity, $\bar{v}_w$. The rigorous definition of mean free path is

$$\bar{\lambda}_w = \frac{\lambda_\infty \int_o^\infty n(v) \; \dfrac{G\left(\dfrac{v + U_\infty}{\bar{v}_\infty}\right)}{(v + U_\infty)} \; v^3 \, d\omega \, dv}{\int_o^\infty n(v) \; v^2 \, d\omega \, dv} \tag{28}$$

where $n(v)$ is the number density of reemitted molecules in velocity-position coordinates and is given by Eq. (12). The term $d\omega \, v^2 \, dv$ is the elemental volume in velocity space.

For hypersonic flows, $\dfrac{v + U_\infty}{\bar{v}_\infty} \gg 1$. Therefore, from Fig. 11,

$$G\left(\frac{v + U_\infty}{\bar{v}_\infty}\right) \simeq \sqrt{2}$$

If the body is highly cooled, $v \ll U_\infty$ over most of the range of v and the term $(v + U_\infty)$ can be replaced by U_∞. Evaluating the mean free path of reflected molecules for highly cooled bodies in hypersonic flow gives, from Eq. (28),

$$\bar{\lambda}_w = \lambda_\infty \; \frac{\sqrt{2}}{U_\infty} \sqrt{\frac{9\pi}{8} \; \frac{k \, T_w}{m}} \tag{29}$$

This result is the same as that obtained from Eq. (24) after assuming the conditions of hypersonic flow and a highly cooled body. For conditions other than the highly cooled body in a hypersonic stream it will be assumed that the mean free path of reemitted molecules as given by Eq. (24) is applicable.

3.2.4 Aerodynamic Drag in Near-Free-Molecular Flow

In the near-free-molecular flow regime the number of free-stream molecules striking the surface is diminished from the free-molecular value because some have been deflected by molecules reemitted from the body. In order to facilitate a discussion of molecular collisions, velocity distribution of molecules, and other properties of molecules, it is desirable to divide the molecules into various classes according to their past history. The undisturbed medium through which the body is moving is identified by the subscript ∞. Molecules that have been reflected from the wall and have not experienced a collision with molecules of a different class are given the subscript w. Molecules that actually strike the surface are known as incident molecules, i. In the near-free-molecule region it will be assumed that the incident molecules are composed of

16

molecules from the free stream that have not undergone a collision with
molecules emitted from the wall prior to impacting upon the surface.
Free-stream molecules and molecules from the wall that collide with
each other are shifted into the class of scattered molecules, s.

In the near-free-molecule flow analysis that follows, it is assumed
that a free-stream molecule is put in the scattered class only by a col-
lision with a molecule from the wall, and that scattered molecules do not
contribute to the drag of the sphere. In other words, the shielding effect
of the molecules emitted from the sphere is the only effect considered.

Two analytical approaches have been attempted for the near-free-
molecule flow regime. One of these is an intuitive approach wherein the
effects of collisions between molecules emitted from the body and free-
stream molecules are considered. This is the so-called first-collision
method. The other approach is an attempt to approximate the solution of
the Boltzmann equation for a body in near-free-molecule flow. Among the
noteworthy investigations are those of Baker and Charwat (Ref. 9) who
followed the first-collision method and that of Willis (Ref. 10) who obtained
an iterative solution of the Boltzmann equation. A semiempirical method
for the transitional region has been proposed by Rott and Whittenbury
(Ref. 11). The results of these studies will be discussed briefly below.

Baker and Charwat (Ref. 9) consider the first collision of molecules
reflected from a sphere with free-stream molecules. The equation they
obtained for C_D is

$$C_D = 2 \left[1 + \frac{\bar{v}_e}{v_o} (0.444) - B(0.23) - \frac{\bar{v}_e}{v_o} B(0.65) \right] \tag{30}$$

where terms of order B^2 have been neglected. Retaining these terms,
their analysis gives

$$C_D = 2 \left\{ 1 + \frac{\bar{v}_e}{v_o} (0.444) - B \left[0.386 \left(\frac{\bar{v}_e}{v_o} \right)^2 + 0.637 \frac{\bar{v}_e}{v_o} + 0.23 \right] \right.$$
$$\left. + B^2 \left[0.566 \left(\frac{\bar{v}_e}{v_o} \right)^2 + 0.181 \frac{\bar{v}_e}{v_o} - 0.007 \right] \right\} \tag{31}$$

where B and $\bar{v}_e/v_o$ are, as calculated by the present authors,

$$B = 1/Kn_w$$

and

$$\frac{\bar{v}_w}{U_\infty} \equiv \frac{\bar{v}_e}{v_o} = \frac{3}{4} \sqrt{\frac{2\pi}{\gamma}} \left(\frac{1}{M_\infty} \right) \sqrt{\frac{T_w}{T_\infty}} \tag{32}$$

17

This expression for $\bar{V}_e/V_o$ is obtained if $\bar{V}_e$ is assumed to be the average velocity of molecules passing a plane in a gas at a temperature of T_w. This value of $\bar{V}_e/V_o$ gives the correct free-molecular value of C_D for the case of $\beta \to 0$. The value obtained in Baker and Charwat's paper is

$$\frac{\bar{V}_e}{V_o} = \left(\frac{3}{\gamma}\right)^{1/2} \left(\frac{1}{M_\infty}\right) \left(\frac{T_w}{T_\infty}\right)^{1/2}$$

which apparently is based upon a value for $\bar{V}_e$ of $\sqrt{3RT_w}$ or the root mean square of the velocity of gas molecules contained in a volume of gas at a temperature equal to T_w. It is necessary to use Eq. (32) in order to obtain the correct free-molecule limit.

Willis (Ref. 10) obtained a near-free-molecular approximation to the Boltzmann equation and applied it to obtain the drag coefficient of a sphere. He considered the solution for both hard sphere molecules and Maxwellian molecules and found, for Maxwell molecules,

$$C_D = 2 \left[1 + \frac{0.59}{S_b} - a \left(0.37 + \frac{2.0}{S_b} \right) \right] \tag{33}$$

and, for hard sphere molecules,

$$C_D = 2 \left[1 + \frac{0.59}{S_b} - a \left(0.37 + \frac{3.2}{S_b} \right) \right] \tag{34}$$

In terms of this paper,

and

$$\left. \begin{aligned} S_b &= \sqrt{\gamma/2} \; M_\infty \; \sqrt{T_\infty/T_w} \\[2mm] a &= \frac{\sqrt{\gamma} \; M_\infty}{4 \, Kn_\infty} \sqrt{\frac{T_\infty}{T_w}} \end{aligned} \right\} \tag{35}$$

This value of a is appropriate only for the hard sphere molecular model. However, for comparison, this definition of a will be used in the drag equation for the Maxwell molecules.

For hypersonic flow Eq. (25) may be simplified to

$$Kn_w = \frac{Kn_\infty \sqrt{2}}{1 + M_\infty \sqrt{\frac{8\gamma}{9\pi} \left(\frac{T_\infty}{T_w}\right)}} \tag{36}$$

Equation (36) may be used with Eq. (35) to express a in terms of Kn_w.

Rott and Whittenbury (Ref. 11) assume that the flow in the transitional region can be represented by a two-component fluid. One component is treated as a molecular beam, whereas the other component is treated as a continuum fluid. Their method is semiempirical in the sense that the two extremes, i. e., the free molecular and the inviscid value of C_D, are obtained from experiment. They obtain an expression for C_D of the form

$$C_D = C_{D_i} + e^{-C_3/Kn_\infty} (C_{D_{fm}} - C_{D_i})$$ (37)

where C_1 is a "free" constant to make the equation best fit the experimental data.

In a discussion of kinetic theory it is assumed that the dynamics of a molecule are independent of its past history. To be more specific, it is assumed that the probability of a molecule undergoing a collision within the next instant of time is not a function of the time since the last collision. Let $a(v) \, d\ell$ be the probability that a molecule moving with velocity v in the direction of ℓ will collide with other molecules within the distance $d\ell$.

Instead of looking at only one molecule and giving odds on its being in a collision, we can consider a large number of molecules and determine the distribution of collisions with other molecules as a function of length. Consider a large number of molecules, $N(0)$, leaving a point, $\ell = 0$, with velocity, v, in the direction of a coordinate axis, ℓ. The $N(0)$ molecules are emitted at intervals of time large enough to prevent interference with each other. $N(\ell)$ is the number of the emitted group of molecules at a distance ℓ from the initial point that have not experienced a collision.

The number of molecules that undergo a collision between ℓ and $\ell + d\ell$ can be expressed as the product of the number of molecules at ℓ and the probability that a single molecule will have a collision in $d\ell$. This may be written as

$$N(\ell) \, a(v) \, d\ell$$ (38)

The number of colliding molecules can also be regarded as the negative of the rate of change of $N(\ell)$ along the direction of motion times the incremental length, i. e.,

$$- [dN(\ell)/d\ell] \, d\ell$$ (39)

Equating quantities (38) and (39) yields the relation

$$- [dN(\ell)/d\ell] \, d\ell = N(\ell) \, a(v) \, d\ell$$ (40)

19

Solving this differential equation and applying the boundary condition that $N(\ell) = N(0)$ at $\ell = 0$ gives

$$N(\ell) = N(0) \ e^{-a(v)\ell} \tag{41}$$

The mean free path of molecules with speed, v, is

$$\lambda(v) = \frac{\int_0^\infty -\ell \left(\frac{dN}{d\ell}\right) d\ell}{\int_0^\infty -\frac{dN}{d\ell} d\ell}$$

which reduces to

$$\lambda(v) = 1/a(v) \tag{42}$$

Jeans (Ref. 33) gives the mean free path of gas molecules as a function of their velocity relative to a static gas. His result is presented as a curve in Fig. 11. The equation of this curve is

$$G\left(\frac{v}{v_\infty}\right) \equiv \frac{\lambda(v)}{\lambda_\infty} = \frac{8 \ \sqrt{2} \ \left(\frac{v}{v_\infty}\right)^2}{\pi \left\{ \frac{v}{v_\infty} \left(\frac{4}{\pi}\right) e^{-4(v/\overline{v}_\infty)^2/\pi} + \left[\frac{8}{\pi} \left(\frac{v}{v_\infty}\right)^2 + 1\right] \mathrm{erf} \left[\frac{v}{\overline{v}_\infty} \left(\frac{2}{\pi}\right)\right] \right\}} \tag{43}$$

It is assumed that the mean free path of molecules reflected from a wall is equal to the mean free path of a molecule with velocity $\overline{v}_w$, where $\overline{v}_w$ is the mean velocity of molecules emitted from the wall. This mean free path will be designated λ_w. The number of molecules that experience a collision between distances of ℓ and $\ell + d\ell$ from the wall is therefore

$$N(0) \ e^{-\ell/\lambda_w} \ \frac{d\ell}{\lambda_w} \tag{44}$$

This expression will be used to obtain the total number of collisions between reemitted and free-stream molecules at a point in space.

If the mean free path of gas molecules reflected from the surface is very large compared to the sphere diameter, but still finite, a molecule leaving the model can be considered to originate from a point source. A simplified analysis will follow in which it is assumed that the sphere can be considered a point source. A more comprehensive analysis is undertaken in the next section wherein the finite size of the sphere is taken into account.

By determining the relative number of collisions per unit time between free-stream molecules and molecules from the wall, the number

20

of free-stream molecules that become incident molecules can be deter-
mined. Since it is assumed that incident molecules are composed of
only free-stream molecules that have not experienced a collision, the
drag coefficient of the sphere is simply

$$C_D = C_{D_{fm}} \frac{n_i}{n_\infty} \qquad (45)$$

in the near-free-molecule regime.

Consider the molecules leaving a surface, dA, within a solid angle,
$d\omega$. These molecules will remain within this solid angle until they under-
go a collision with another molecule. The distribution of collisions of
these $N^{(0)}$ molecules is given by Eq. (43). The number of molecules
within $d\omega$ must be determined by an integration over the sphere surface.

As developed earlier, the number of molecules from each element
of surface area, dA, within $d\omega$ is, from Eq. (13),

$$n_w \left(\frac{2kT_w}{m}\right)^{1/2} \frac{\cos\phi \; d\omega \; dA}{2(\pi)^{3/2}}$$

where n_w is given by Eq. (17). Confining attention to the reflected mole-
cules which are directed upstream into the incident flow, ϕ and θ may be
considered identical, as shown in the following sketch:
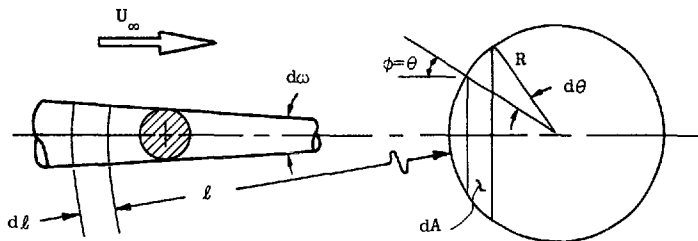
By reference to the sketch it is seen that

$$dA = 2\pi R^2 \sin\theta \; d\theta$$

21

Integrating over the front surface of the sphere, the total number of molecules directed upstream within $d\omega$ is

$$\left(\frac{2kT_i}{m}\right)^{1/2} \frac{d\omega R^2 n_i}{\sqrt{\pi}} \int_0^{\pi/2} \left\{ e^{-(S\cos\theta)^2} + \sqrt{\pi}\,(S\cos\theta)\Big[1 + \text{erf}\,(S\cos\theta)\Big] \right\} \sin\theta \cos\theta\, d\theta =$$

$$(46)$$

$$\left(\frac{2kT_i}{m}\right)^{1/2} \frac{d\omega R^2 n_i}{\sqrt{\pi}\,S^2} \left[\frac{1}{6} - \frac{e^{-S^2}}{6} + \frac{S^2}{3} e^{-S^2} + \frac{1}{3}\sqrt{\pi}\,S^3 + \frac{\sqrt{\pi}\,S^3}{3}\,\text{erf}\,S \right]$$

The number of collisions per unit volume per unit time at a distance ℓ from the sphere is the number of collisions per unit time within $d\omega$ from ℓ to $\ell + d\ell$ divided by the volume of the space within $d\omega$ from ℓ to $\ell + d\ell$. This volume is $(\ell + R)^2\, d\omega\, d\ell$.

The expression for the number of collisions between free-stream and reemitted molecules per unit volume per unit time may be written as

$$\eta = \left(\frac{2kT_i}{m}\right)^{1/2} \frac{R^2 n_i}{\sqrt{\pi}\,(\ell + R)^2} \left[\frac{1}{6S^2} - \frac{e^{-S^2}}{6S^2} + \frac{e^{-S^2}}{3} + \frac{1}{3}\sqrt{\pi}\,S + \frac{\sqrt{\pi}\,S}{3}\,\text{erf}\,S \right] \frac{e^{-\ell/\overline{\lambda}_w}}{\overline{\lambda}_w}$$

$$(47)$$

Since the number of free-stream molecules and the number of wall molecules colliding are equal, the number per unit time of free-stream molecules prevented from impact upon the sphere can be determined by integrating the above expression from $\ell = \infty$ to the surface, $\ell = 0$, i.e.,

$$(n_\infty - n_i)\, U_\infty = \int_0^\infty \eta\, d\ell \tag{48}$$

Integrating Eq. (48), using Eq. (47) for η, gives

$$(n_\infty - n_i)\, U_\infty = \left[\frac{1}{6S^2} - \frac{e^{-S^2}}{6S^2} + \frac{e^{-S^2}}{3} + \frac{\sqrt{\pi}\,S}{3} + \frac{\sqrt{\pi}\,S}{3}\,\text{erf}\,S \right] \tag{49}$$

$$\left\{ \frac{R}{\lambda_w} - \left(\frac{R}{\lambda_w}\right)^2 e^{R/\lambda_w} \left[-\,\text{Ei}\left(-\,\frac{R}{\lambda_w} \right) \right] \right\} \left(\frac{2kT_i}{m} \right)^{1/2} \frac{n_i}{\sqrt{\pi}}$$

where $-\,\text{Ei}\,(-R/\lambda_w)$ is the exponential integral (Ref. 36).

Since it is assumed that the probability of a free-stream molecule being in a collision is independent of the thermal random velocity distribution, then T_i is equal to T_∞. Using this equality and the expression for

S, Eq. (49) becomes

$$\frac{1 - \frac{n_i}{n_\infty}}{\frac{n_i}{n_\infty}} = \left(\frac{1}{6 S^3} - \frac{e^{-S^2}}{6 S^3} + \frac{e^{-S^2}}{3 S} - \frac{\sqrt{\pi}}{3} + \frac{\sqrt{\pi}}{3} \text{ erf } S \right)$$

$$\left\{ \frac{R}{\lambda_w} - \left(\frac{R}{\lambda_w} \right)^2 e^{R/\lambda_w} \left[- Ei \left(- \frac{R}{\lambda_w} \right) \right] \right\} \frac{1}{\sqrt{\pi}}$$

$$(50)$$

From Eqs. (45) and (50) it is found that

$$\frac{C_D}{C_{D_{fm}}} = \frac{n_i}{n_\infty} = \frac{1}{\frac{f(S)}{\sqrt{\pi}} \left\{ \frac{R}{\lambda_w} - \left(\frac{R}{\lambda_w} \right)^2 e^{R/\lambda_w} \left[- Ei \left(- \frac{R}{\lambda_w} \right) \right] \right\} + 1} \qquad (51)$$

where

$$f(S) = \frac{1}{6 S^3} - \frac{e^{-S^2}}{6 S^3} + \frac{e^{-S^2}}{3 S} + \frac{1}{3} \sqrt{\pi} + \frac{\sqrt{\pi}}{3} \text{ erf } S \qquad (52)$$

And, from Ref. 35, $C_{D_{fm}}$ is given by

$$C_{D_{fm}} = \frac{2 S^2 + 1}{\sqrt{\pi} S^3} e^{-S^2} + \left(\frac{4 S^4 + 4 S^2 - 1}{2 S^4} \right) \text{ erf } S + \frac{2 \sqrt{\pi}}{3 S} \sqrt{\frac{T_w}{T_\infty}} \qquad (53)$$

Equations (51), (52), and (53) can be used to obtain a drag coefficient of a sphere in the near-free-molecular regime where $d \ll \lambda_w$. If the mean free path of the reemitted molecule is on the order of the sphere diameter, then the assumption that the sphere may be treated as a point source is not justified. In the remainder of this section an analysis is made wherein the finite size of the sphere is considered. It is assumed in the following analysis that the Mach number is large. Other assumptions are the same as those in the preceding analysis.

The number of collisions per unit volume per unit time at a point in space involving molecules which emanate from a surface element dA is

$$d\eta = \frac{n_w \left(\frac{2 k T_w}{m} \right)^{1/2} \cos \phi}{2 \pi^{3/2} \lambda_w \ell^2} e^{-\ell/\lambda_w} dA \qquad (54)$$

where n_w is given by Eq. (17). For large values of S (large Mach number), n_w becomes

$$n_w = n_i \sqrt{\frac{T_i}{T_w}} (2 \sqrt{\pi} S \cos \theta) \qquad (55)$$

23

In order to get the total number of collisions per unit volume per unit time at a point P, Eq. (54) must be integrated over the surface elements of the body that "see" the point in space.

It is assumed that the sphere is in a uniform free-molecule flow composed of the incident molecules. The number density of this incident flow can be determined at the stagnation point of the sphere. The following sketch shows a point on the centerline ahead of the stagnation point of a sphere and related notation:
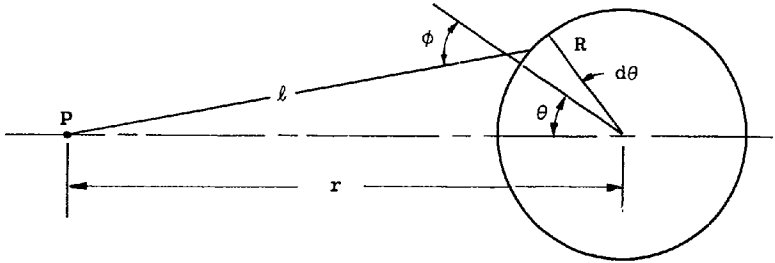
Since the flow is axially symmetric, the element of area dA in Eq. (54) may be written as

$$2 \pi R^2 \sin \theta \, d\theta$$

The collision density involving molecules reemitted from this area is

$$d\eta = \frac{n_w}{\sqrt{\pi}} \left(\frac{2 k T_w}{m} \right)^{1/2} \frac{\cos \phi \, R^2 \, \sin \theta}{\lambda_w \, \ell^2} \, e^{-\ell/\overline{\lambda}_w} \, d\theta \qquad (56)$$

This expression must be integrated over values of θ from $\theta = 0$ to $\phi = \pi/2$. The total collision rate density at P is therefore

$$\eta = \int_{\theta = 0}^{\phi = \pi/2} \frac{n_w}{\sqrt{\pi}} \left(\frac{2 k T_w}{m} \right)^{1/2} \frac{\cos \phi \, R^2 \, \sin \theta}{\lambda_w \, \ell^2} \, e^{-\ell/\overline{\lambda}_w} \, d\theta \qquad (57)$$

In order to evaluate this integral, it is convenient to express all variables in terms of ℓ/λ_w. From the law of cosines for triangles with sides ℓ, r, R, it is seen that

$$\ell^2 = r^2 + R^2 - 2r \, R \, \cos \theta \qquad (58)$$

24

and

$$r^2 = \ell^2 + R^2 - 2 \ell R (- \cos \phi) \qquad (59)$$

Differentiating Eq. (58) gives

$$\sin \theta \; d\theta = (\ell / r R) \; d\ell \qquad (60)$$

Let

$$\ell / \lambda_w = A \quad \text{when} \quad \phi = \pi/2$$

and

$$\ell / \lambda_w = B \quad \text{when} \quad \theta = 0$$

It is observed that

$$A = \sqrt{\left(\frac{r}{\lambda_w}\right)^2 - \left(\frac{R}{\lambda_w}\right)^2} \qquad (61)$$

and

$$B = r/\lambda_w - R/\lambda_w \qquad (62)$$

Substituting Eqs. (55), (58), (59), (60), (61), and (62) into Eq. (57) gives the result,

$$\eta = \int_B^A \left\{ \frac{n_i}{2} \left(\frac{S}{\lambda_w}\right)\left(\frac{2kT_i}{m}\right)^{1/2} \Big/ \left[\left(\frac{r}{\lambda_w}\right)^2 \; \frac{R}{\lambda_w} \left(\frac{\ell}{\lambda_w}\right)^2\right]\right\} \left[\left(\frac{\ell}{\lambda_w}\right)^2 - \left(\frac{r}{\lambda_w}\right)^2 - \left(\frac{R}{\lambda_w}\right)^2\right] \qquad (63)$$

$$\left[\left(\frac{\ell}{\lambda_w}\right)^2 + \left(\frac{R}{\lambda_w}\right)^2 - \left(\frac{r}{\lambda_w}\right)^2\right] e^{-\ell/\lambda_w} \; d\left(\frac{\ell}{\lambda_w}\right)$$

Equation (63) may be written as

$$\eta = \frac{n_i \; U_\infty}{2\lambda \left(\frac{r}{\lambda_w}\right)^2 \left(\frac{R}{\lambda_w}\right)} \int_B^A \frac{\left[\left(\frac{\ell}{\lambda_w}\right)^4 - 2\left(\frac{\ell}{\lambda_w}\right)^2 \left(\frac{r}{\lambda_w}\right)^2 + \left(\frac{r}{\lambda_w}\right)^4 - \left(\frac{R}{\lambda_w}\right)^4\right] e^{-\ell/\lambda_w} \; d\left(\frac{\ell}{\lambda_w}\right)}{\left(\frac{\ell}{\lambda_w}\right)^2} \qquad (64)$$

Evaluating the integral in Eq. (64), one finds

$$\eta = \frac{n_i \; U_\infty}{2\lambda_w \left(\frac{r}{\lambda_w}\right)^2 \left(\frac{R}{\lambda_w}\right)} \left\{ e^{-B} \; (B^2 + 2B + 2) - e^{-A} \; (A^2 + 2A + 2) - 2\left(\frac{r}{\lambda_w}\right)^2 \right. \qquad (65)$$

$$\left. (e^{-B} - e^{-A}) + \left[\left(\frac{r}{\lambda_w}\right)^4 - \left(\frac{R}{\lambda_w}\right)^4\right]\left\{\frac{e^{-B}}{B} - \left[-\text{Ei}\,(-B)\right] - \frac{e^{-A}}{A} + \left[-\text{Ei}\,(-A)\right]\right\}\right\}$$

Equation (65) is presented graphically in Fig. (12) where $\eta \lambda_w/(n_i U_\infty)$ is plotted as a function of $r/\lambda_w - R/\lambda_w$ for various values of R/λ_w.

Using Eqs. (45) and (48), it is found that

$$\frac{C_D}{C_{D_{fm}}} = \frac{1}{1 - \frac{1}{n_i \, v_\infty} \int_0^\infty \eta \, d\ell} \tag{66}$$

The integral in Eq. (66) was evaluated numerically.

Application of Eqs. (66), (25), and (53) to calculate the drag coefficients corresponding to conditions in the LDH Tunnel shows that C_D is underestimated, though not as badly as when earlier theories are used. However, it is important to realize that the greater part of the experimental data lie outside the first-collision regime. Comparison of Eq. (66) with the earlier theories represented by Eqs. (29), (30), (33), (34), and (37) reveals that all are in close agreement concerning the initial departure of C_D from the free-molecular limit. When lower Knudsen numbers are considered, the theories diverge most rapidly, with Eq. (66) showing closer agreement with the data as well as a form which is more similar to the trend of the data toward the limit corresponding to near-inviscid flow.

A degree of uncertainty exists because of unresolved questions, such as those pertaining to the free-stream intermolecular force field, degrees of accommodation, and manner of reflection, plus the neglect of scattered molecules and collisions subsequent to the first. For example, the assumption of specular reemission results in the present theory being in closer agreement with experiment, as also does the assumption of less than complete accommodation.

Following from the observation of the satisfactory form of Eq. (66) and in view of the uncertainties mentioned above, the authors chose the factor of proportionality in Eq. (27) to achieve a matching of Eq. (66) and the experimental, hypersonic, cold-wall data. This factor was found to be 2.446, i.e.,

$$Kn_w \text{ (mod.)} = 2.446 \, \frac{\sqrt{\gamma} \, M_\infty}{Re_\infty} \tag{67}$$

The present and all the other theories reviewed herein are compared with the new data in Fig. 13 where Kn_w (mod.) is used as defined by Eq. (67). Use of the factor 2.446 improves agreement of all theories with the data, but most of the earlier theories still indicate much too rapid a decrease of drag as Knudsen number decreases. The theory represented by Eq. (37), it will be recalled, already includes a free constant chosen to best fit the present data, but it underestimates the extent of the transition between near-inviscid and near-free-molecular flows. Since the factor introduced in Eq. (67) and Fig. 13 probably may be regarded as a constant for hypersonic, cold-wall conditions, its use is thought to be justified.

26

As an aid in the further examination of the validity of Eq. (66), it is compared with experimental data corresponding to $2 < M_\infty < 11$ in Fig. 14. There it may be seen that all data are reasonably well correlated by the chosen parameters at high Knudsen numbers. * Also, although points corresponding to low Mach numbers are not plentiful at the higher Knudsen numbers, it may be seen that Eqs. (66) and (67) with the factor 2.446 treated as a constant may be a satisfactory approximation at the higher Knudsen numbers, even for Mach number as low as two.

4.0 DISCUSSION AND CONCLUSIONS

First of all, it would appear that a semiempirical approximation to the drag coefficient is capable of closely matching the experimentally determined data to nearly the free-molecular flow regime. The provisional values of the coefficients in the approximation,

$$C_D = C_{D_i} + K_1/\sqrt{Re_2} + K_2/Re_2$$

appear to be functions of Mach number and heat transfer to the spheres in perfect gases. At Mach numbers above six, the heat-transfer condition becomes more important than Mach number. Values given for K_1 and K_2 in the hypersonic, cold-wall condition are believed to be more accurate than those for low Mach numbers, largely because of the stronger possibility of model support and base pressure influences in the latter case. It is shown that K_2 is negative.

The new first-collision type of analysis presented herein is shown to produce an equation for sphere drag coefficient which possesses several attractive features. It is not limited to very high Mach numbers and cold walls, and it yields a drag coefficient at the limit, $Kn \to 0$, which is on the order of the known, continuum, near-inviscid value. Use of an experimentally determined factor, which probably may be regarded as a constant for high Mach numbers and cold walls, causes the present theory to fit experimental data satisfactorily at Reynolds numbers far beyond the first-collision regime. Equation (66) with the modification of Eq. (67) is shown in Fig. 15 to effect the correspondence of the continuum to the non-continuum analytical results, thus offering a means for determining drag of spheres under the conditions specified and throughout the entire range of Reynolds or Knudsen numbers encountered.

*The data would approach different limits as Knudsen numbers approached zero, since $C_{D_i}/C_{D_{fm}} \neq$ const. for $2 < M_\infty < 11$.

REFERENCES

1. Kane, E. C. "Drag Forces on Spheres in Low Density Supersonic Gas Flow." University of California Report No. HE-150-65, February 15, 1950.

2. Sherman, Frederick, S. "Note on Sphere Drag Data." Journal of the Aeronautical Sciences, Vol. 18, No. 8, August 1951, p. 566.

3. Jensen, N. A. "Supplementary Data on Sphere Drag Tests. Part 2." University of California Report No. HE-150-92, Sept. 11, 1951.

4. May, A. "Supersonic Drag of Spheres at Low Reynolds Numbers in Free Flight." Journal of Applied Physics, Vol. 28, 1957, pp. 910-912.

5. Masson, D. J., Morris, D. N., and Bloxsom, Daniel E. "Measurements of Sphere Drag from Hypersonic Continuum to Free-Molecule Flow." Rand Corporation Research Memorandum RM-2678, Nov. 3, 1960.

6. Wegener, Peter P. and Ashkenas, Harry. "Wind Tunnel Measurements of Sphere Drag at Supersonic Speeds and Low Reynolds Numbers." Journal of Fluid Mechanics, Vol. 10, Part 4, June 1961, pp. 550-560.

7. Potter, J. L., Kinslow, M., Arney, G. D., Jr., and Bailey, A. B. "Description and Preliminary Calibration of a Low-Density, Hypervelocity Wind Tunnel." AEDC-TN-61-83, Aug. 1961.

8. Sreekanth, A. K. "Drag Measurements on Circular Cylinders and Spheres in the Transition Regime at a Mach Number of 2." University of Toronto UTIA Report No. 74, April 1961.

9. Baker, R. M. L., Jr. and Charwat, A. F. "Transitional Corrections to the Drag of a Sphere in Free Molecule Flow." The Physics of Fluids, Vol. 1, No. 2, March-April 1958, pp. 73-81.

10. Willis, D. R. "Study of Nearly Free-Molecule Flow." Aerodynamics of the Upper Atmosphere. Project Rand Report R-339, Paper No. 13, June 1959.

11. Rott, Nicholas and Whittenbury, Clive G. "A Flow Model for Hypersonic Rarefied Gasdynamics with Applications to Shock Structure and Sphere Drag." Douglas Aircraft Co. Report SM-38524, May 12, 1961.

12. Shamberg, R. "Analytical Representation of Surface Interaction for Free Molecular Flow with Application to Drag of Various Bodies." Rand Corp. Report R-339, Sect. 12, June 1959.

13. Chahine, M. "Similarity Solution for Stagnation Point Heat Transfer in Low-Density, High-Speed Flow." Research Summary No. 36-8, Jet Propulsion Laboratory, May 1, 1961, pp. 82-84.

14. Sentman, Lee H. "Free Molecule Flow Theory and Its Application to the Determination of Aerodynamic Forces." Lockheed Missiles and Space Div. Technical Report LMSD-448514, October 1, 1961.

15. Ashkenas, H. I. "Sphere Drag at Low Reynolds Numbers and Supersonic Speeds." Research Summary No. 36-12, Jet Propulsion Laboratory, January 2, 1962, pp. 93-95.

16. Aroesty, Jerome. "Sphere Drag in Low Density Supersonic Flow." University of California Report No. HE-150-192, January 3, 1962.

17. Potter, J. Leith and Boylan David E. "Experience with an Over-expanded Nozzle in a Low-Density, Hypervelocity Wind Tunnel." AEDC-TDR-62-85, April 1962.

18. Arney, George D., Jr. and Boylan, David E. "A Calorimetric Investigation of Some Problems Associated with a Low-Density, Hypervelocity Wind Tunnel." (AEDC-TDR to be published).

19. Svehla, Roger A. "Estimated Viscosities and Thermal Conductivities of Gases at High Temperatures." NASA TR R-132, 1962.

20. Rott, Nicholas and Lenard, Michael. "Vorticity Effect on the Stagnation-Point Flow of a Viscous Incompressible Fluid." Journal of the Aerospace Sciences, Vol. 26, No. 8, August 1959, pp. 542-543.

21. Van Dyke, Milton. "Higher Approximations in Boundary-Layer Theory." Lockheed Missiles and Space Div., LMSD-'.03097, October 1960.

22. Van Dyke, Milton. "Second-Order Boundary-Layer Theory for Blunt Bodies in Hypersonic Flow." American Rocket Society International Hypersonics Conf. Preprint No. 1966-61, August 1961.

23. Cohen, Clarence B. and Reshotko, Eli. "Similar Solutions for the Compressible Laminar Boundary Layer with Heat Transfer and Pressure Gradient." NACA Report 1293, 1956.

24. Hodges, A. J. "The Drag Coefficient of Very High Velocity Spheres." Journal of the Aeronautical Sciences, Vol. 24, No. 10, Oct. 1957, pp. 755-758.

25. Lehnert, Richard. "Base Pressure of Spheres at Supersonic Speeds." NAVORD Report 2774, February 4, 1953.

26. Kavanau, L. L. "Base Pressure Studies in Rarefied Supersonic Flows." Journal of the Aeronautical Sciences, Vol. 23, No. 3, March 1956, pp. 193-207, 230.

27. Van Dyke, M. "Second-Order Compressible Boundary-Layer Theory with Application to Blunt Bodies in Hypersonic Flow." AFOSR-TN-61-1270 (AD-267859), July 1961.

28. Hayes, Wallace D. and Probstein, Ronald F. Hypersonic Flow Theory. Academic Press, 1959, p. 372.

29. Ferri, Antonio, Zakkay, Victor, and Ting, Lu. "Blunt-Body Heat Transfer at Hypersonic Speed and Low Reynolds Numbers." Journal of the Aerospace Sciences, Vol. 28, No. 12, Dec. 1961, pp. 962-971, 991.

30. Wachman, Harold W. "The Thermal Accommodation Coefficient: A Critical Survey." American Rocket Society Journal, Vol. 32, No. 1, Jan. 1962, pp. 2-12.

31. Schaaf, S. A. and Chambré, P. L. "Flow of Rarefied Gases." Fundamentals of Gas Dynamics. Ed. Howard W. Emmons, Princeton, New Jersey, 1958, p. 697.

32. Kennard, Earle H. Kinetic Theory of Gases. McGraw-Hill Book Company, Inc., New York and London 1938, p. 62.

33. Jeans, J. H. The Dynamical Theory of Gases. Dover Publications, Inc., pp. 256-257. (Fourth Edition).

34. Probstein, Ronald F. "Shock Wave and Flow Field Development in Hypersonic Re-Entry." American Rocket Society. Paper presented at the ARS Semi-Annual Meeting, Los Angeles, Calif., May 9-12, 1960.

35. Stalder, Jackson R. and Zurick, Vernon J. "Theoretical Aerodynamic Characteristics of Bodies in a Free-Molecule-Flow Field." NACA TN-2423, July 1951.

36. National Bureau of Standards. Tables of Sine, Cosine and Exponential Integrals, Vols. I and II. Federal Works Agency, Works Progress Administration, 1940.

TABLE 1

CONDITIONS AND RESULTS OF THE LDH WIND TUNNEL FREE-FALL TESTS

h_w/h_o	T_w/T_∞	M_∞	Diameter, in.	Re_∞	Re_2	$C_{D_{fm}}$	C_D	$C_D/C_{D_{fm}}$
0.076	2.00	10.6	0.0312	9.40	1.08	2.21	1.94	0.877
	2.00	10.6		9.46	1.09		2.02	0.912
	2.00	10.6	0.0392	11.95	1.38		1.99	0.899
	2.00	10.6		11.86	1.37		1.94	0.874
	2.00	10.6		11.86	1.37		1.88	0.849
	1.98	10.5	0.0469	14.46	1.69		1.90	0.859
	2.00	10.6		14.19	1.64		1.94	0.874
	2.00	10.6	0.0625	18.92	2.19		1.87	0.846
	2.05	10.7	0.0781	23.07	2.64		1.76	0.794
	2.01	10.6		23.49	2.71		1.78	0.805
0.086	2.29	10.7	0.0312	10.74	1.18	2.22	2.03	0.914
	2.25	10.6		11.01	1.23		1.95	0.878
	2.26	10.6		10.95	1.22		1.94	0.874
	2.28	10.7	0.0392	13.54	1.49		1.92	0.862
	2.26	10.6		13.74	1.52		1.98	0.891
	2.28	10.7	0.0469	16.20	1.78		1.93	0.868
	2.24	10.6		16.60	1.86		1.94	0.870
	2.26	10.7	0.0625	21.81	2.41		1.85	0.834
	2.28	10.7		21.59	2.37		1.99	0.896
	2.24	10.6		22.13	2.40		1.88	0.847
	2.26	10.7		21.81	2.38		1.86	0.838
	2.24	10.6		22.13	2.48		1.82	0.820
	2.29	10.7	0.0781	26.85	2.94		1.68	0.756
	2.24	10.6		27.95	3.14		1.69	0.761
	2.28	10.8	0.0938	31.89	3.47		1.65	0.741
	2.30	10.7		32.06	3.50		1.68	0.753
	2.30	10.7		32.06	3.50		1.69	0.762
	2.26	10.7		32.72	3.62		1.69	0.758
	2.24	10.6		33.37	3.74		1.62	0.728
	2.24	10.6		33.55	3.77		1.63	0.732
	2.25	10.6		33.03	3.68		1.72	0.774
	2.24	10.6		33.55	3.77		1.61	0.723

TABLE 1 (Concluded)

h_w/h_0	T_w/T_∞	M_∞	Diameter, in.	Re_∞	Re_2	$C_{D_{fm}}$	C_D	$C_D/C_{D_{fm}}$
0.086	2.30	10.7	0.1250	42.75	4.66	2.22	1.60	0.717
	2.30	10.7		42.75	4.66		1.68	0.754
	2.25	10.6		44.04	4.91		1.56	0.703
	2.29	10.7	0.1562	53.72	5.88		1.55	0.696
	2.25	10.6		55.05	6.14		1.56	0.700
	2.24	10.6		55.61	6.23		1.61	0.724
	2.29	10.7	0.1875	64.45	7.05		1.55	0.696
	2.31	10.8	0.2188	74.07	8.03		1.50	0.674
	2.29	10.7	0.2500	53.70	9.40		1.48	0.667
	2.26	10.7	0.2812	98.16	10.86		1.44	0.646
	2.30	10.7	0.3125	106.87	11.66		1.42	0.638
	2.30	10.7	0.3438	117.56	12.82		1.42	0.638
	2.28	10.7	0.3750	129.57	14.21		1.36	0.609
0.121	3.03	10.5	0.0312	13.65	1.38	2.26	2.07	0.918
	3.03	10.5		13.65	1.38		2.00	0.886
	3.06	10.6		13.42	1.35		1.89	0.839
	3.03	10.5		13.65	1.38		1.96	0.870
	3.03	10.5	0.0392	17.12	1.73		1.97	0.871
	3.03	10.5	0.0625	27.19	2.75		1.79	0.794
	3.03	10.5		27.19	2.75		1.86	0.825
	3.03	10.5	0.0781	33.99	3.44		1.81	0.799
	3.04	10.6	0.0938	40.62	4.10		1.79	0.790
	3.03	10.5	0.1250	54.39	5.50		1.65	0.732
	3.04	10.6	0.1562	67.71	6.83		1.61	0.714
0.154	3.97	10.7	0.0312	14.61	1.48	2.29	2.06	0.902
	3.99	10.8	0.0392	18.25	1.83		2.04	0.892
	3.96	10.7	0.0625	29.35	2.99		1.91	0.834
	3.99	10.8		29.09	2.92		1.95	0.851
	4.00	10.8	0.0781	36.24	3.62		1.92	0.826
	3.98	10.8	0.0938	43.66	4.42		1.74	0.761
	3.96	10.7	0.1250	58.71	5.98		1.64	0.716
	3.96	10.7	0.1562	73.38	7.47		1.63	0.713
	3.97	10.7		73.21	7.42		1.58	0.691
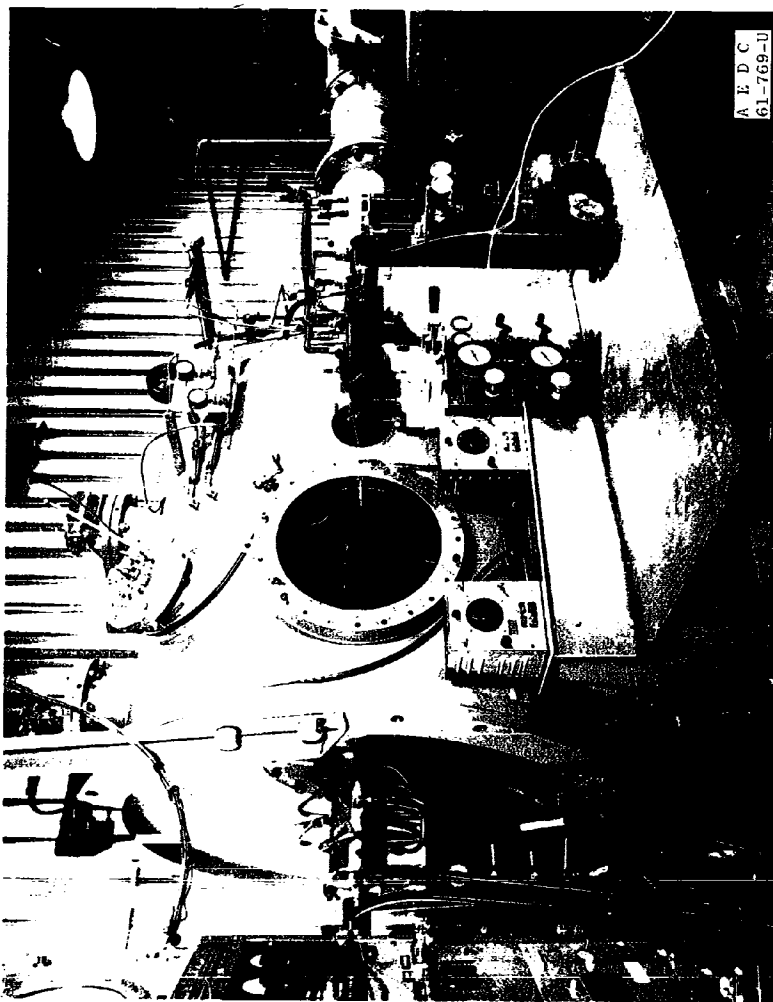
Fig. 1 The Low-Density, Hypervelocity Wind Tunnel

33
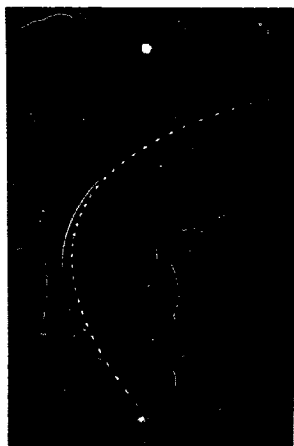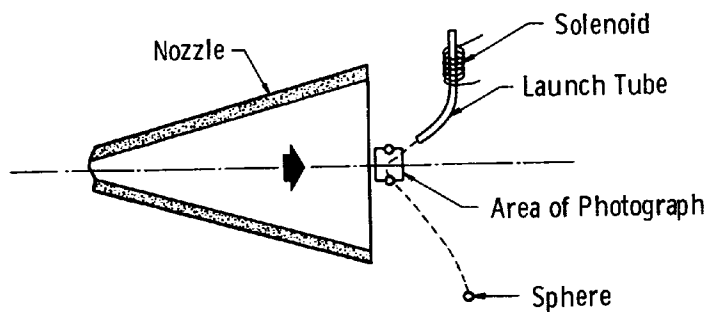
Fig. 2 Typical Trajectory of Sphere during Free Flight through Test Section
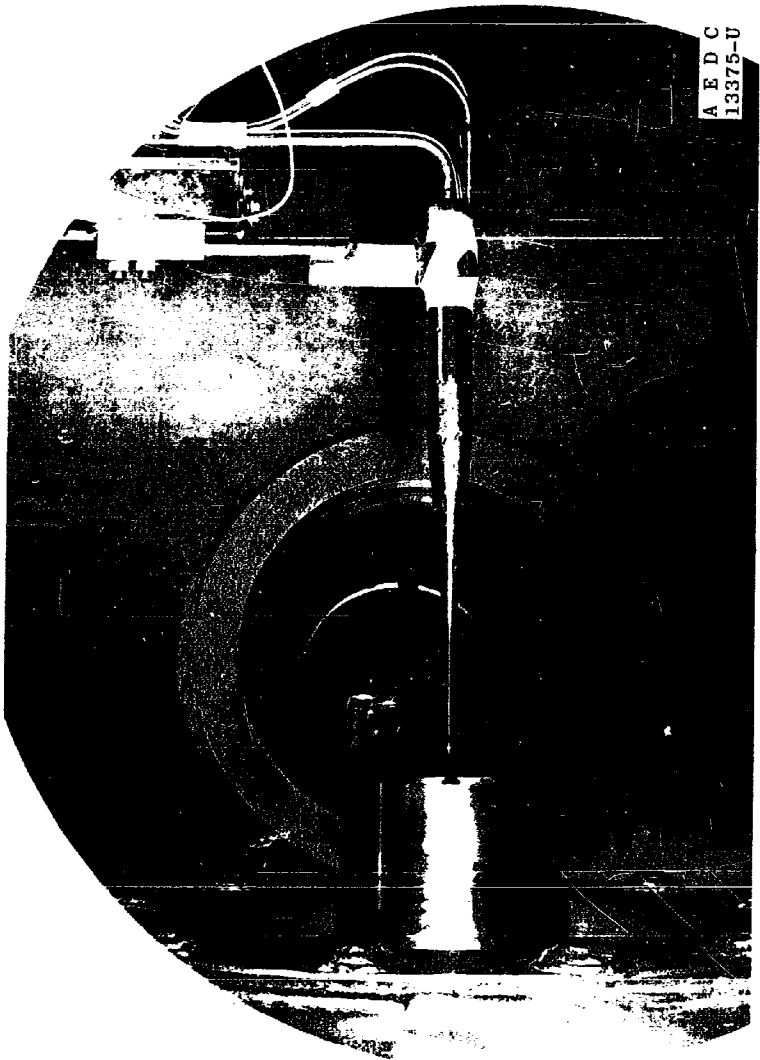
Fig. 3 Drag Balance Installed in the LDH Wind Tunnel

A E D C
13375-U
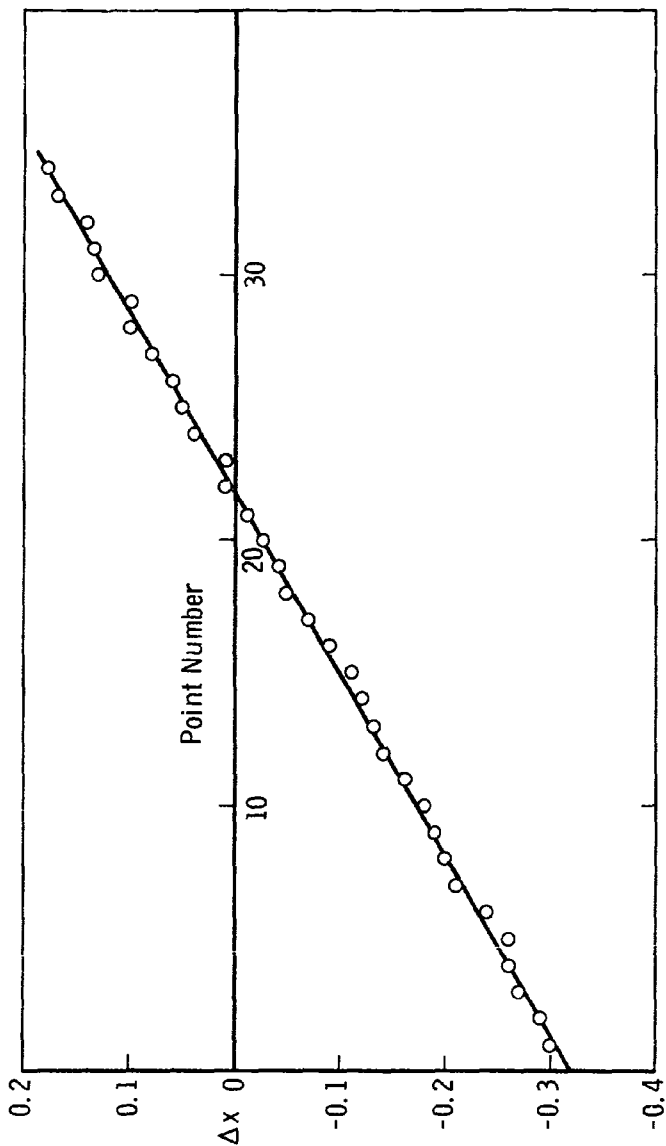
Fig. 4 Axial Displacement of Sphere as a Function of Data Point Number
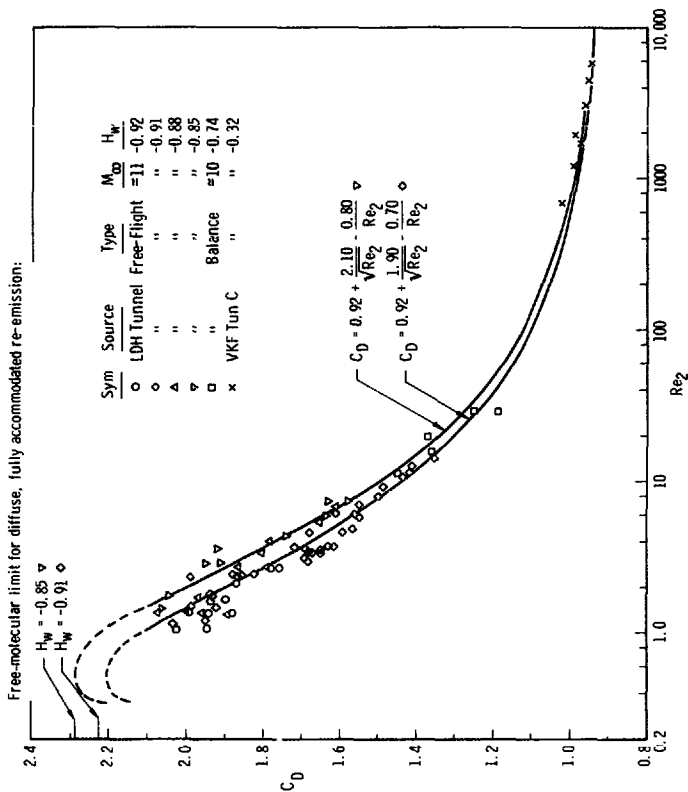
Fig. 5 Drag of Spheres in Hypersonic Flow with $h_w < h_o$: New Data
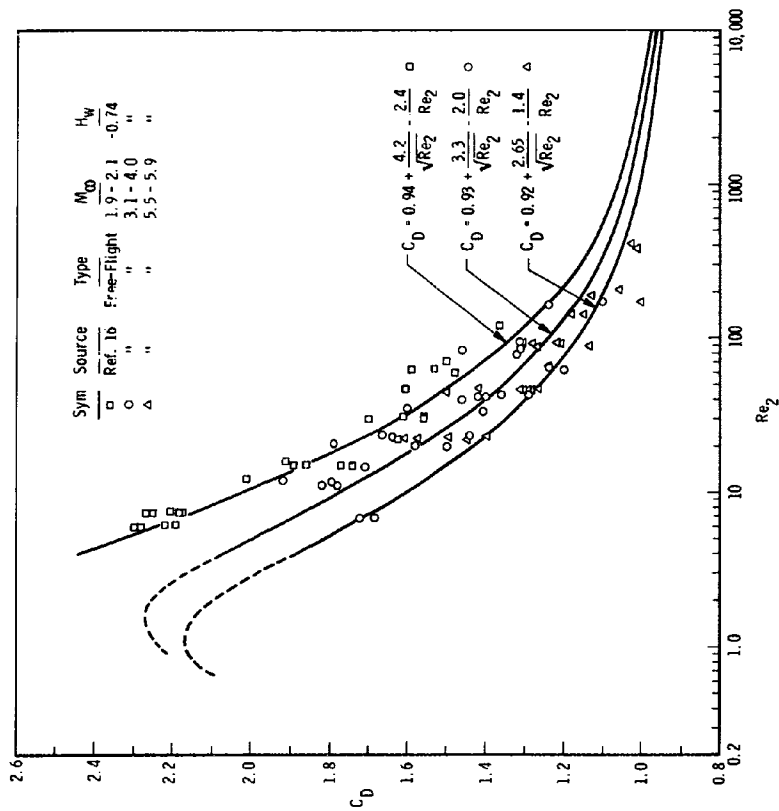
Fig. 6 Drag of Spheres in Supersonic Flow with $h_w < h_o$
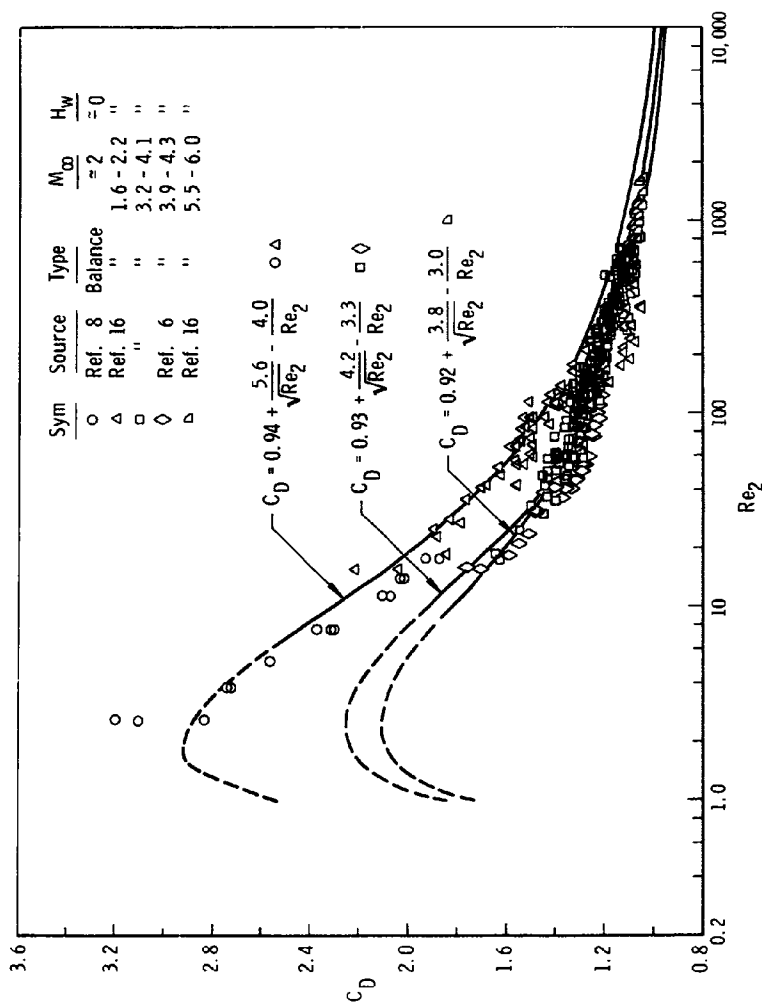
Fig. 7 Drag of Spheres in Supersonic Flow with $h_w \cong h_o$
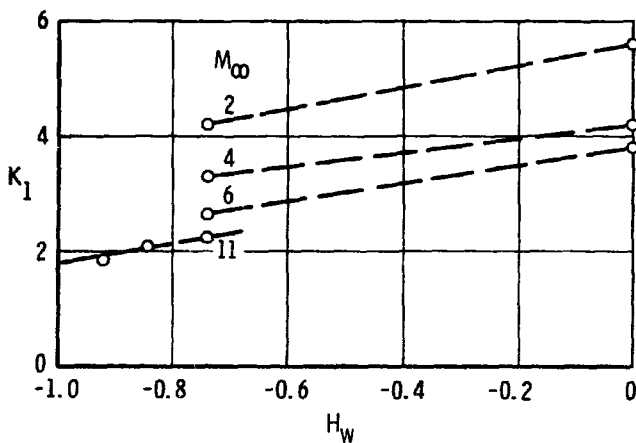
Fig. 8 Provisional Values of K_1
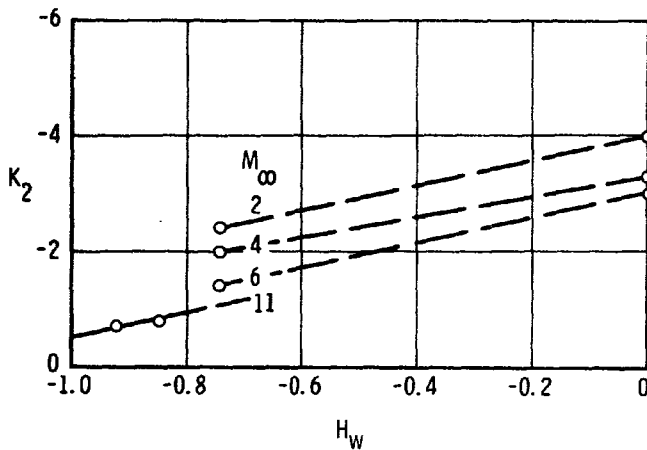
Fig. 9 Provisional Values of K_2
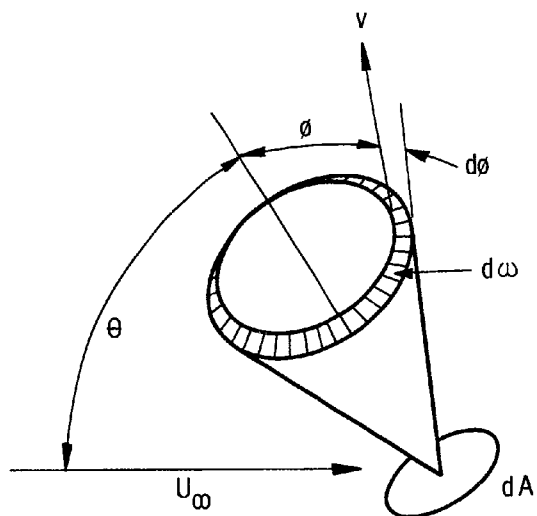
Fig. 10 Nomenclature Used for Incident and Reemitted Molecules
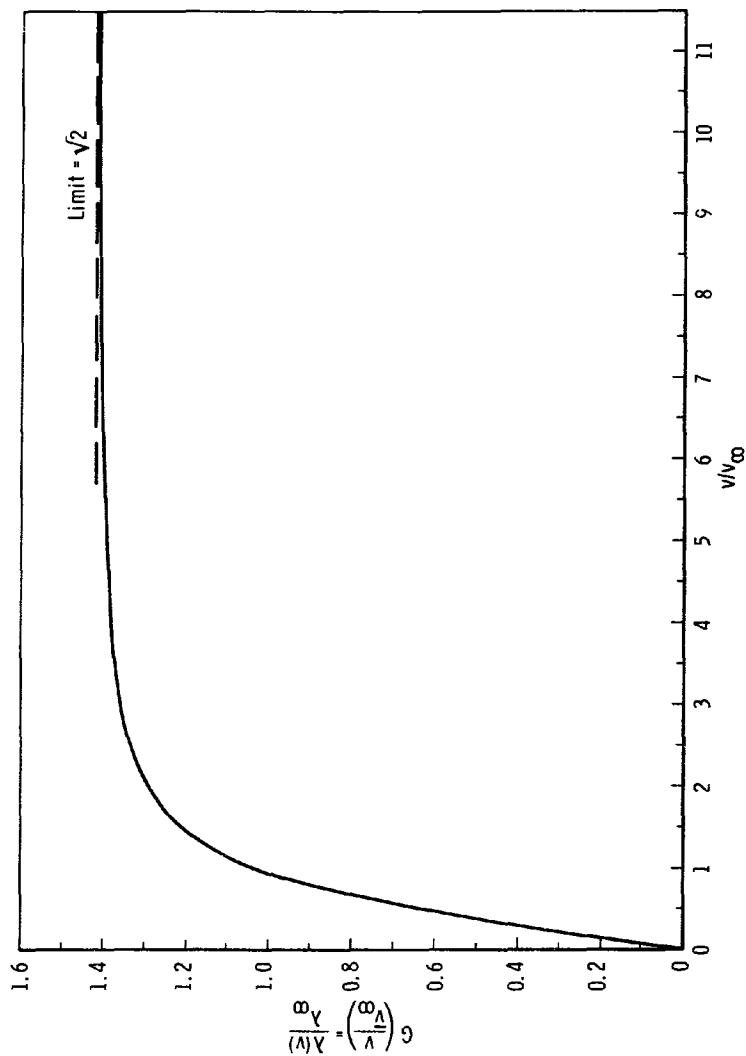
Fig. 11 Mean Free Path as a Function of Velocity
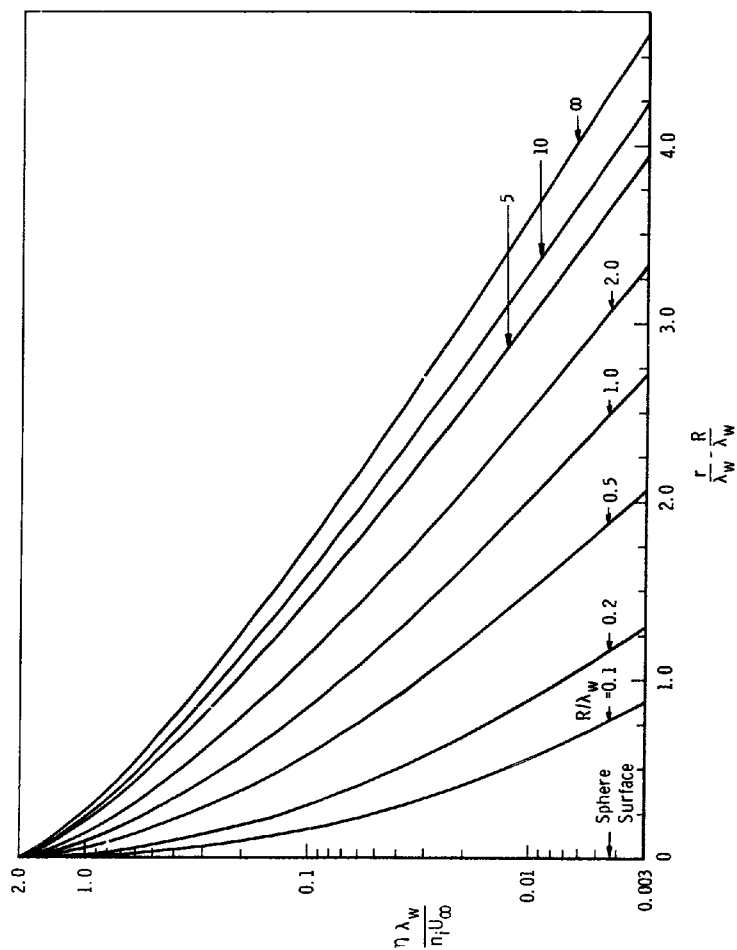
Fig. 12 Collision Rate Density ahead of Stagnation Point, Eq. (65)
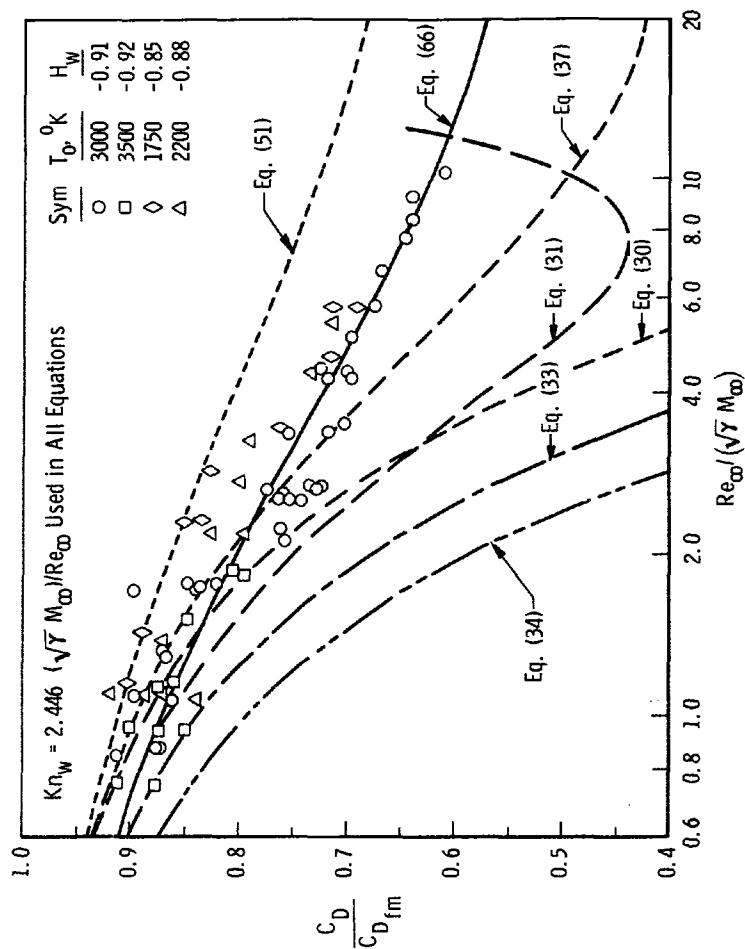
Fig. 13 Comparison of Theories and LDH Wind Tunnel Data for the Hypersonic, Cold-Wall Condition
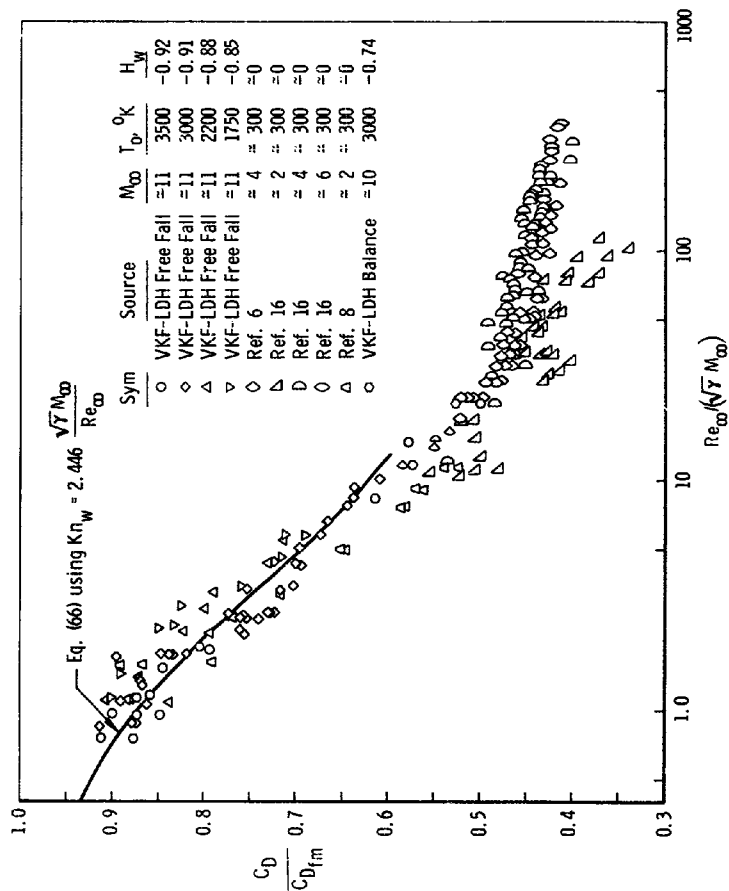
Fig. 14 Comparison of Hypersonic Theory with Hypersonic and Supersonic Data

45
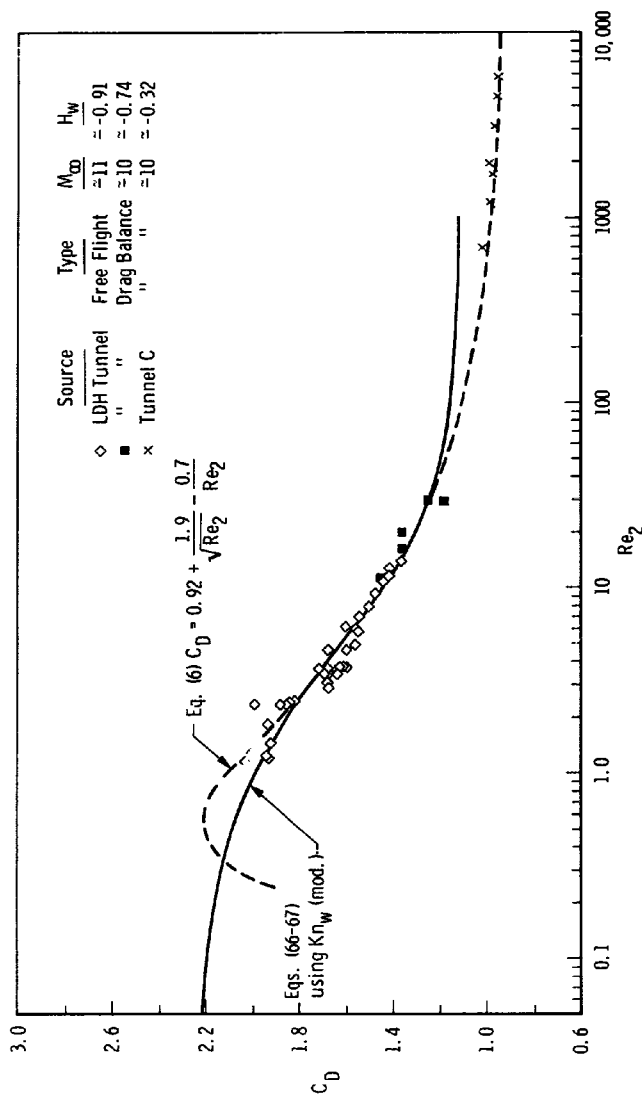
Fig. 15 Region of Correspondence of Results from Continuum and Noncontinuum Analyses. Equations for $M_\infty \approx 11$ and $H_w \approx -0.91$

Arnold Engineering Development Center
Arnold Air Force Station, Tennessee
Rpt. No. AEDC-TDR-62-205. THE DRAG OF SPHERES
IN RAREFIED HYPERVELOCITY FLOW. December 1962,
58 p. incl 36 refs., illus., table. Unclassified Report

Through use of the low-density, hypervelocity wind tunnel of
the von Kármán Gas Dynamics Facility, drag of spheres has
been measured under hypersonic, cold-wall $(T_w \ll T_0)$,
support-free conditions in a nonreacting (vibration frozen)
flow. Data were obtained for a nominal free-stream Mach
number of 11 and for Reynolds numbers from 1 to 10 based
on conditions immediately downstream of the bow shock and
sphere diameter. These data were supplemented by meas-
urements at a nominal Mach number of 10 where a conven-
tional balance was used, and Reynolds numbers downstream
of the shock as high as 10^4 were investigated in the cold-
wall condition. The experimental results have been ana-
lyzed both from the point of view of continuum flow with
second-order viscous effects, and from the standpoint of a
noncontinuum concept, taking account of first collisions
between reemitted and free-stream molecules. In the
former case, a drag coefficient representation of the form

$C_D = C_{D_{FM}} (1 + K_1/\sqrt{Re_2} + K_2/Re_2$, is shown to fit the data
very closely when K_1 and K_2 are allowed to be functions of
free-stream Mach number and wall-to-total-enthalpy ratio.
Data from investigations at the University of California,
University of Toronto, and Jet Propulsion Laboratory have
been used to enlarge the present study and, in particular, to
support the evaluation of K_2 which represents the influences
of vorticity, curvature, thick boundary layer, slip, and
temperature jump. In all cases, K_1 was found to be negative
in sign. The new first-collision analysis is numerically
indeterminant because of the lack of a method for explicit
calculation of mean free path in real, polyatomic gases with
consideration of intermolecular forces. However, the form
of the derived equation for $C_D/C_{D_{FM}}$ agrees appears to fit
the experimental data over a considerable range of Knudsen
numbers if a free constant is used in the expression for
mean free path. It is considered that this constant is in-
fluenced by the type of intermolecular and gas-solid inter-
actions occurring. Fully accommodated, diffusely
reflected surface interaction was assumed in the analysis.

1. Hypervelocity flow
2. Spheres
3. Drag
4. Analysis
5. Superaerodynamics
I. AFSC Program Area 750A,
   Project 8953. Task 895306
   Contract AF 40(600)-1000
II. ARO, Inc., Arnold AF Sta.,
   Tenn.
IV. Max Kinslow and
   J. L. Potter
V. Available from OTS
VI. In ASTIA Collection